

1 Towards reducing the high cost of parameter sensitivity analysis in 2 hydrologic modelling: a regional parameter sensitivity analysis 3 approach

4

5 Samah Larabi¹, Juliane Mai², Markus Schnorbus¹, Bryan A. Tolson², Francis Zwiers¹

6 ¹Pacific Climate Impacts Consortium, University of Victoria, Victoria, British Columbia, Canada

7 ²University of Waterloo, Department of Civil and Environmental Engineering, Waterloo, Ontario, Canada

8 *Correspondence to:* Samah Larabi (slarabi@uvic.ca)

9 **Abstract.** Land surface models have many parameters that have a spatially variable impact on model outputs. In applying
10 these models, sensitivity analysis (SA) is sometimes performed as an initial step to select calibration parameters. As these
11 models are applied on large domains, performing sensitivity analysis across the domain is computationally prohibitive. Here,
12 using a VIC deployment to a large domain as an example, we show that watershed classification based on climatic attributes
13 and vegetation land cover helps to identify the spatial pattern of parameter sensitivity within the domain at a reduced cost. We
14 evaluate the sensitivity of 44 VIC model parameters with regard to streamflow, evapotranspiration and snow water equivalent
15 over 25 basins with a median size of 5078 km². Basins are clustered based on their climatic and land cover attributes.
16 Performance of transferring parameter sensitivity between basins of the same cluster is evaluated by the *FI* score. Results
17 show that two donor basins per cluster are sufficient to correctly identify sensitive parameters in a target basin, with *FI* scores
18 ranging between 0.66 (evapotranspiration) to 1 (snow water equivalent). While climatic attributes are sufficient to identify
19 sensitive parameters for streamflow and evapotranspiration, including vegetation class significantly improves skill in
20 identifying sensitive parameters for snow water equivalent. This work reveals that there is opportunity to leverage climate and
21 land cover attributes to greatly increase the efficiency of parameter sensitivity analysis and facilitate more rapid deployment
22 of land surface models over large spatial domains.

23 1 Introduction

24 Land surface models (LSMs) are often used over large-scale domains (i.e., continental, or subcontinental river basins) to
25 analyze hydrologic variables of interest. The main purpose of large-domain hydrologic modelling is to simulate, in a spatially
26 consistent manner, the processes governing water fluxes across different geographic and hydroclimatic regions (Mizukami et
27 al., 2017). The application of LSMs over large domains raises several challenges, including the availability of driving data and
28 observations for calibration and the computational cost of calibration.

29 Parameter estimation when modelling the hydrology of large domains is particularly challenging due the number of parameters
30 that must be estimated, the resulting computational demand and the impact of spatial heterogeneity on parameter
31 transferability. Given the lack of guidance on parameter transferability over large domains, LSMs often rely on a priori
32 parameterizations based on expert opinion, case studies, field data, or hydrologic theory (Beck et al., 2016, Rakovec et al.,
33 2019). Specifically, LSM parametrization of vegetation and soil characteristics is generally based on other measured
34 characteristics or found in the literature from soil and vegetation classes (Nasonava et al., 2009). This approach relies on the
35 assumption that vegetation and soil type solely determine the ideal values of vegetation parameters and soil parameters
36 respectively, neither of which is supported by previous studies (e.g., Rosero et al., 2010; Cuntz et al., 2016; Bennett et al.,
37 2018).

38 LSM parameter estimation is a high dimensional problem (Göhler et al, 2013; Cuntz et al., 2016). The calibration parameter
39 space can, however, be reduced by a sensitivity analysis (SA) that serves to identify parameters that strongly influence the
40 model output variance. SA provides objective insights on calibration parameters by eliminating parameters from the
41 calibration space that do not affect model output variance (hereafter called noninformative parameters) and reducing the
42 probability of over-parameterization (Van Griensven et al., 2006; Cuntz et al., 2015; Demirel et al., 2018). The computational
43 cost of SA depends on the number of model runs needed to simulate realistic model responses, which increases significantly
44 with the number of model parameters considered (Sarrazin et al., 2016; Devak and Dhanya, 2017). Therefore, SA of LSMs is
45 either overlooked and calibration parameters are selected based on the expert judgement and/or a previous SA, or when
46 performed, the list of model parameters analyzed is artificially shortened to exclude numerous model parameters whose values
47 are not known with certainty. Recent sensitivity analysis studies of LSMs, have however, revealed the impact of fixed-value
48 parameters (i.e., parameters assigned fixed values, often within the model code itself) on model output variance (e.g., Mendoza
49 et al., 2015; Cuntz et al., 2016; Houle et al., 2017), thus raising the need to explore and estimate these parameters to improve
50 the spatial accuracy of LSM outputs and the representation of hydrologic processes.

51 Sensitivity analysis studies show that parameter sensitivities vary geographically depending on the hydroclimatic conditions
52 (Demaria et al., 2007; Gou et al., 2020) and considered hydrologic processes (Bennett et al., 2018; Sepúlveda et al., 2021). As
53 land surface models are often applied on increasingly larger domains, performing sensitivity analysis across the entire domain
54 to identify the spatial pattern of sensitive parameters becomes increasingly computationally prohibitive, particularly when one
55 considers the large number of parameters involved. In addition, there is a lack of guidance in the literature on ways to
56 extrapolate parameter sensitivity from local to the larger scale with a reduced computational cost.

57 One approach for extrapolating parameter sensitivity is watershed classification, which aims at identifying watersheds that are
58 similar in some sense (i.e., according to certain attributes). Hydrological applications of watershed classification include
59 understanding general catchment hydrologic behavior (e.g., Sawicz et al., 2011), estimation of flow duration curves and
60 streamflow in ungauged sites (e.g., Boscarello et al., 2016; Kanishka and Eldho, 2020) and estimation of environmental model

61 parameters in scarce data regions (e.g., Jafarzadegan et al., 2020). In this paper, we investigate the utility of watershed
62 classification for reducing the cost of large-scale parameter sensitivity.

63 Our objective is to demonstrate the application of watershed classification as a means to regionalize parameter sensitivity. We
64 do this using an example deployment of the Variable Infiltration Capacity model (VIC, Liang et al., 1994, 1996). The VIC
65 model has been extensively used for regional hydrological modelling, but with typically only 4 to 11 parameters adjusted
66 during calibration (e.g., Wenger et al. 2010; Shreshta et al., 2012; Oubeidillah et al., 2013; Schnorbus et al., 2014; Islam et al.,
67 2017; Lohmann et al., 1998; Nijssen et al., 2001; Xie and Yuan, 2006; He and Pang, 2014; Melsen et al., 2016; Yanto et
68 al., 2017; Ismail et al., 2020; Gou et al., 2020; Waheed et al., 2020). Nevertheless, many additional VIC parameters that are
69 typically fixed also affect model output variance (e.g., Mendoza et al., 2015; Melsen et al., 2016; Houle et al., 2017; Bennett
70 et al., 2018). Hence, we examine the regionalization of parameter sensitivity for a much larger suite of 44 parameters that
71 includes 14 soil parameters, four climate parameters, six snow-related parameters, three glacier parameters and 17 vegetation
72 related parameters. In order to address a range of hydrologic processes, parameter sensitivity is assessed with regard to three
73 model outputs: streamflow, evapotranspiration and snow water equivalent.

74 This paper is organized as follows. Section 2 describes the study area, the VIC-GL model and its parametrization, the sequential
75 screening method and the watershed classification approach used. Section 3 presents the results of the sensitivity analysis for
76 streamflow, evapotranspiration, snow cover, and the results of transferring parameter sensitivity based on watershed
77 classification. Section 4 provides a discussion of the results followed by conclusions in Sect. 5, where we also discuss the
78 implications for cost effective sensitivity analysis when considering hydrologic models with large numbers of parameters that
79 are deployed across large domains.

80 **2 Methods**

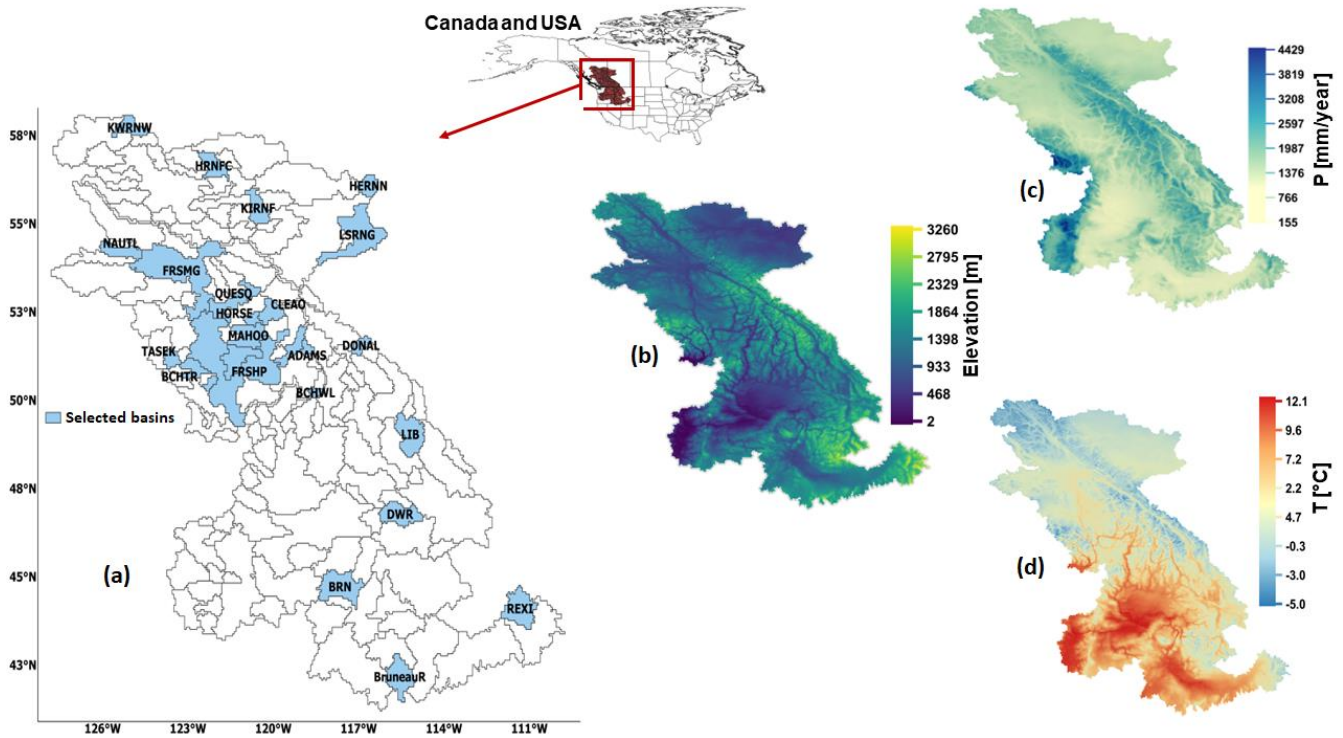
81 Section 2.1 presents the study area and the dataset used to drive the VIC-GL model. Section 2.2 describes the version of VIC
82 used here, while Sec. 2.3 describes its parametrization and initialization. The parameter sampling strategy is also described in
83 Sect. 2.3. Section 2.4 presents the Efficient Elementary Effects (EEE; Morris, 1991) screening method used to identify VIC-
84 GL informative parameters. Section 2.5 presents the physical similarity approach used to transfer parameter importance to
85 other basins.

86 **2.1 Study area and dataset**

87 The study area extends over the Pacific Northwest region of North America from 40.75° N to 57.6° N and 109.96° W to 127.9°
88 W (see Fig.1). It encompasses three large watersheds, the Peace, Fraser and Columbia rivers, with a combined area of
89 1,150,624 km². This region spans many physiographic and climatic zones, resulting in substantial hydroclimatic spatial
90 variability. The domain was subdivided into several smaller basins (158 in total) according to location of hydrometric gauges.

91 We selected 25 of these basins representing glacierized conditions in the Coast Mountains and the Rocky Mountains, semi-
 92 arid conditions in the interior of both the Fraser and Columbia and in eastern Peace, and the arid conditions of the southern
 93 Columbia. The location of these basins is presented in Fig. 1 and their characteristics are summarised in Table 1 and 2. The
 94 selected basins capture large spatial variability in precipitation, which is largely controlled by orography, such that average
 95 annual precipitation over the 25 basins ranges from 337 mm/year to 1666 mm/year. The sampled basins also capture a strong
 96 latitudinal gradient of air temperature, with average annual temperature ranging from $-0.37\text{ }^{\circ}\text{C}$ to $7.43\text{ }^{\circ}\text{C}$. The snow index, the
 97 fraction of annual precipitation that falls as snow when temperature is below 2°C (Woods, 2009; Sawicz et al., 2011), ranges
 98 from 0.38 to 0.70. The aridity index, the ratio of evapotranspiration to precipitation (ET/P), ranges from 0.28 to 1.66. Average
 99 catchment elevation ranges from 683 m to 1990 m.

100



101

102 **Figure 1: Modelled domain with the location of the 25 selected sub-basins (a), the domain digital elevation map (b), mean annual**
 103 **precipitation (c) and mean annual temperature (d), which were calculated from the PNWNmet dataset.**

104

105

106

108 **Table 1: Physiographic attributes of 25 selected basins.**

Basin ID	Basin name	Basin description	Area [km²]	Glacier area [km²]	Average elevation [m]	Relief [m]
1	ADAMS	Adams River near Squilax, BC	3130	41	1266	1558
2	BCHTR	Bridge River at Terzaghi Dam, BC	2745	54	1748	1434
3	BCHWL	Shuswap River at Wilsey Dam, BC	1021	0	1339	1208
4	BONAP	Bonaparte River below Cache Creek, BC	5334	0	1216	1305
5	BRN	Snake River at Brownlee Dam, Idaho/Oregon	8877	0	1299	1692
6	CAYOO	Cayoosh Creek near Lilloet, BC	954	2	1770	1400
7	CLEAO	Clearwater River at the outlet of Clearwater Lake, BC	3031	224	1625	1540
8	DONAL	Columbia River at Donald, BC	1623	115	1767	1838
9	DWR	North Fork Clearwater River at Dworshak Dam, ID	6066	0	1307	1341
10	FRSHP	Fraser River at Hope, BC	31557	62	1198	2015
11	FRSMG	Fraser near Marguerite, BC	20810	0	867	968
12	HERNN	Krawchuk Drainage near McLennan, BC	4018	0	683	160
13	HORSE	Horsefly River above McKinley Creek, BC	1242	0	1400	990
14	KIRNF	Kiskatinaw River near Farmington, BC	6196	0	910	555
15	LIB	Kootenai River at Libby Dam, MT	6977	0	1327	1240
16	LSRNG	Little Smoky River near Guy, AB	18975	0	868	946
17	MAHOO	Maood River at outlet of Mahood Lake, BC	5078	0	1194	1072
18	NAUTL	Nautley river near Fort Fraser, BC	3163	0	956	565
19	QUESQ	Quesnel River near Quesnel, BC	5551	78	1251	1442
20	SEYMO	Seymour River near Seymor Arm, BC	1024	41	1516	1422
21	TASEK	Taseko River at outlet of Taseko Lake, BC	1789	194	1990	1098
22	REXI	Henry's Fork Rexburg, ID	8034	0	1983	1590
23	BurneauR	Bruneau River near Hot Spring, Idaho	7074	0	1711	1852
24	KWRNW	Kwadacha River Near Ware, BC	5034	144	1538	1433
25	HRNFC	Halfway River near Farrel Creek, BC	5906	0	835	705

110 The climatic attributes presented in Table 2 are spatially averaged by sub-basin from the gridded PNWNAmet dataset (Werner
 111 et al., 2019), which is used to drive the VIC model. This dataset provides gridded observations of daily precipitation (mm) and
 112 minimum and maximum temperature ($^{\circ}\text{C}$) for the Northwestern North America. The dataset is available at a daily timestep
 113 and a spatial resolution of $1/16^{\circ}$ for the period 1945 to 2012. Wind speed (m/s) from the 20CR reanalysis (Compo et al., 2011)
 114 that has been spatially interpolated to $1/16^{\circ}$ is also provided with the PNWNAmet dataset at a daily timescale. For further
 115 details see Werner et al. (2019).

116 **Table 2: Climatic attributes of the 25 selected basins.**

Basin name	Average annual precipitation [mm]	Average annual temperature [$^{\circ}\text{C}$]	Snow index	Aridity index
ADAMS	1196	3.39	0.47	0.40
BCHTR	1123	1.42	0.62	0.37
BCHWL	991	3.64	0.51	0.48
BONAP	475	3.88	0.43	1.04
BRN	557	7.42	0.40	1.01
CAYOO	995	1.93	0.60	0.43
CLEAO	1492	1.00	0.57	0.28
DONAL	1194	0.23	0.61	0.34
DWR	1271	5.88	0.48	0.41
FRSHP	951	3.96	0.44	0.51
FRSMG	634	2.94	0.44	0.76
HERNN	448	1.23	0.47	1.14
HORSE	1119	2.17	0.51	0.40
KIRNF	575	2.19	0.45	0.87
LIB	856	3.93	0.48	0.56
LSRNG	570	2.62	0.41	0.90
MAHOO	675	3.34	0.45	0.72
NAUTL	583	2.64	0.45	0.82
QUESQ	939	2.86	0.46	0.50
SEYMO	1666	2.63	0.70	0.28
TASEK	1310	-0.37	0.70	0.29
REXI	729	3.54	0.54	0.65
BruneauR	337	7.43	0.38	1.66
KWRNW	845	-1.57	0.62	0.47
HRNFC	514	1.61	0.48	0.96

117 2.2 VIC-GL model

118 VIC is a physically based macroscale model that simulates both water and energy balances by grid cells (Liang et al., 1994,
119 1996; Cherkauer and Lettenmaier, 1999). The VIC model has been widely applied to analyze the impact of climate change on
120 the hydrology and water resources of the study region (e.g., Hamlet and Lettenmaier, 1999; Payne et al., 2004; Shrestha et al.,
121 2012; Schnorbus et al., 2014; Islam et al., 2017) and to study the effect of land cover change on streamflow (e.g., Matheussen
122 et al., 2000). VIC-GL, an upgraded version developed at the Pacific Climate Impacts Consortium (PCIC) that is used here,
123 includes additional functionality to simulate glacier mass balance (Schnorbus, 2018). VIC-GL was branched from VIC version
124 4.2, and although the model physics are in many ways similar, it uses a different model abstraction from its predecessor.
125 Although the computational domain of VIC-GL is still described using a two-dimensional grid (using a spatial resolution of
126 $1/16^\circ$ in the current application), sub-grid variability in land cover and topography uses hydrologic response units (HRUs) as
127 opposed to the original vegetation tiles. Specifically, an HRU is assigned for each land cover class within an elevation band,
128 with the elevation of each HRU being the median of the associated elevation band. In this manner, the type and extent of land
129 cover is allowed to vary with elevation within grid boxes. The vertical water and energy balance is solved separately in each
130 HRU and then averaged to the grid-cell scale. The current application of VIC-GL uses fixed 200-m elevation bands and three
131 soil layers. The baseline model processes are described in detail by Liang et al. (1994, 1996), Cherkauer et al. (2013) and Bohn
132 et al. (2016).

133 Updates to address glacier mass balance modelling are described in detail by Schnorbus (2018), but pertinent VIC-GL
134 parameter changes are summarised here. Glacier surface mass and energy balance modelling introduces three additional
135 parameters *GLAC_ALB*, *GLAC_ROUGH* and *GLAC_REDF*. *GLAC_ALB* specifies the albedo of glacier ice, which controls
136 the amount of incoming solar radiation absorbed by the ice surface. The value of *GLAC_ALB*, once set, is constant in time.
137 The parameter *GLAC_ROUGH* specifies the roughness length of the glacier surface, which affects the wind speed profile and
138 the transfer of energy to the glacier surface due to the turbulent fluxes. The scaling factor for snow redistribution
139 (*GLAC_REDF*) controls the redistribution of precipitation between non-glacier HRUs and acts as a proxy for mechanical snow
140 redistribution that typically occurs via wind and gravity in mountainous alpine environments (e.g. Kuhn 2003). VIC-GL also
141 uses the rain-snow partitioning algorithm of Kienzle (2008) rather than the original algorithm in the VIC model distribution.
142 This is a curvilinear model that uses two parameters, the threshold mean daily temperature (*TEMP_TH_1*), where 50% of
143 precipitation falls as snow, and the temperature range centered on *TEMP_TH_1* within which both solid and liquid precipitation
144 occurs (*TEMP_TH_2*). VIC-GL has also been updated to make certain parameters more accessible for model calibration and
145 to allow for a more spatially explicit description of some hydro-climatic processes. These parameters include five that
146 determine soil albedo decay according to the USACE algorithm (USACE 1956) and the climatic parameters *T_LAPSE* and
147 *PGRAD*. The latter specify vertical temperature and the precipitation gradients that are used to adjust temperature and
148 precipitation, respectively, for each HRU within a grid cell.

149 **2.3 Model parameterization and sampling**

150 We consider 44 VIC-GL parameters (Table 3) composed of 5 baseflow parameters, 1 runoff parameter, 9 drainage parameters,
 151 4 climate parameters, 6 snow-related parameters, 3 glacier parameters and 17 vegetation related parameters. The set of
 152 analyzed parameters includes the commonly calibrated parameters, parameters that have been addressed in previous studies
 153 (e.g., Demaria et al., 2007; Houle et al., 2017; Bennett et al., 2018), and some that are typically set to fixed values (Gao et al.,
 154 2009).

155
 156 **Table 3: The 44 VIC-GL parameters selected for the sensitivity analysis.**

Parameter	Description	Unit	Range	Default	Type*
Baseflow parameters					
ds	Fraction of D _{max} where nonlinear baseflow begins	–	[0.001, 0.6]	0.1	Absolute
dsmax	Maximum velocity of baseflow	mm/day	[1, 200]	40	Absolute
ws	Fraction of maximum soil moisture where nonlinear baseflow occurs	–	[0.4, 1]	0.9	Absolute
c	Exponent used in baseflow curve	–	[1, 10]	2	Absolute
depth3	Thickness of soil layer 3	m	[0.5, 10]	2	Absolute
Runoff parameters					
INFIL	Variable infiltration curve parameter	–	[0.0001, 0.8]	0.2	Absolute
Drainage parameters					
watn	Exponent in Campbell's equation for hydraulic conductivity in all layers	–	[8, 11]	9.5	Absolute
ks	Saturated hydrologic conductivity in all layers	mm/day	[300, 3000]	1081	Absolute
depth1	Thickness of soil layer 1	m	[0.001, 0.5]	0.1	Absolute
depth2	Thickness of soil layer 2	m	[0.05, 1]	0.2	Absolute
bd	Soil bulk density (applied to all layers)	kg/m ³	[800, 1600]	1400	Absolute
sdens	Soil particle density (applied to all layers)	kg/m ³	[2000, 2700]	2500	Absolute
wcr	Critical Point (applied to all layers)	–	[0.35, 0.55]	0.40	Absolute
wppw	Wilting point (applied to all layers)	–	[0.20, 0.50]	0.35	Absolute
resid_moist	Residual moisture (applied to all layers)	–	[0.0, 0.125]	0.08	Absolute
Climate parameters					
PGRAD	Precipitation gradient	1/m	[0.0001, 0.001]	0.0005	Absolute
T_LAPSE	Temperature lapse rate	°C/m	[0, 9.5]	6.5	Absolute

TEMP_TH_1	Rain/snow temperature threshold	°C	parameter 1	[-2.0, 5.0]	2	Absolute
TEMP_TH_2	Rain/snow temperature threshold	°C	parameter 2	[8.0, 15.0]	12	Absolute
Snow parameters						
SNOWROUGH	Surface roughness of snowpack	m		[0.0001, 0.1]	0.01	Absolute
NEW_SNOW_ALB	Albedo of new snow	_		[0.8, 0.9]	0.85	Absolute
SNOW_ALB_ACCUM_A	Albedo decay coefficient during accumulation period	_		[0.3, 0.99]	0.94	Absolute
SNOW_ALB_ACCUM_B	Albedo decay exponent during accumulation period	_		[0, 0.99]	0.58	Absolute
SNOW_ALB_THAW_A	Albedo decay coefficient during thaw period	_		[0.1, 0.99]	0.82	Absolute
SNOW_ALB_THAW_B	Albedo decay exponent during thaw period	_		[0, 0.99]	0.46	Absolute
Glacier parameters						
GLAC_ALB	Albedo of glacier surface	_		[0.2, 0.6]	0.4	Absolute
GLAC_ROUGH	Surface roughness of glacier	m		[0.0001, 0.01]	0.001	Absolute
GLAC_REDF	Scaling factor for snow redistribution with values in range 0 (no redistribution) to 1 (redistribution equal to area ratio)	_		[0, 1]	0	Absolute
Vegetation parameters						
root_depth	Thickness of root zone layer 3	m		[0.5, 2]	1	Multiplicative factor
root_fract1	Fraction of roots in soil layer 1	_		[0, 1]	0.7	Absolute
root_fract2	Fraction of roots in soil layer 2	_		[0, 1]	0.2	Absolute
lai_djf	Leaf Area Index (winter)	m ² /m ²		[0.5, 2]	1	Multiplicative factor
lai_mam	Leaf Area Index (spring)	m ² /m ²		[0.5, 2]	1	Multiplicative factor
lai_jja	Leaf Area Index (summer)	m ² /m ²		[0.5, 2]	1	Multiplicative factor
lai_son	Leaf Area Index (fall)	m ² /m ²		[0.5, 2]	1	Multiplicative factor
alb_dja	albedo(winter)	_		[0.5, 2]	1	Multiplicative factor
alb_mam	albedo(spring)	_		[0.5, 2]	1	Multiplicative factor
alb_jja	albedo(summer)	_		[0.5, 2]	1	Multiplicative factor
alb_son	albedo(fall)	_		[0.5, 2]	1	Multiplicative factor
Rarc	Architectural resistance	s/m		[0.5, 2]	1	Multiplicative factor
Rmin	Minimum stomatal resistance	s/m		[0.5, 2]	1	Multiplicative factor

RGL	Minimum incoming shortwave radiation at which there will be transpiration	W/m ²	[0.5, 2]	1	Multiplicative factor
SolAtn	Solar attenuation factor	_	[0.5, 2]	1	Multiplicative factor
WndAtn	Wind speed attenuation through the overstory	_	[0.5, 2]	1	Multiplicative factor
Trunk_ratio*	Ratio of total tree height that is trunk	_	[-0.2, 0.2]	0	Additive change

157 *Type is the parameter sampling strategy, which is to either replace the parameter default value (i.e., Absolute), apply a
158 multiplicative factor or apply an additive change to the baseline values. The additive change is applied so that trunk ratio
159 remains between 0.1 and 0.8.

160 The commonly calibrated parameters are limited to four baseflow parameters, the runoff parameter, and five drainage
161 parameters. The common baseflow parameters are maximum velocity of baseflow (*dsmax*), fraction of *dsmax* where nonlinear
162 baseflow begins (*ds*), fraction of maximum soil moisture where non-linear baseflow occurs (*ws*) and thickness of deepest soil
163 layer (*depth3*). These parameters describe the non-linear relationship between baseflow rate and soil moisture in the deepest
164 soil layer (with thickness described by *depth3*). The runoff parameter, or variable infiltration curve parameter (*INFIL*),
165 describes the extent of soil saturation within grid cell (i.e., amount of direct runoff) as function of soil moisture in the surface
166 soil layers (i.e., the variable infiltration curve, Liang et al., 1994) which have thicknesses given by *depth1* and *depth2*. The
167 common drainage parameters are the two parameters controlling soil storage capacity (*depth1* and *depth2*), the exponent in
168 Campbell's equation for hydraulic conductivity (*watn*) and the saturated hydrologic conductivity (*ks*).

169 The additional drainage parameters considered are the soil bulk density (*bd*), soil particle density (*sdens*), fractional soil
170 moisture content at the critical point (*wcr*), fractional soil moisture content at the wilting point (*wpwp*) and the residual moisture
171 (*resid_moist*). The *wpwp* parameter dictates baseflow estimation with the ARNO model formulation (Francini and Pacciani,
172 1991) used in VIC (Gao et al., 2009). We also consider the four climate parameters which are temperature lapse rate
173 (*T_LAPSE*), precipitation gradient, and the rain/snow temperature threshold parameter 1 and 2 (*TEMP_TH_1* and
174 *TEMP_TH_2*). The examined parameters also include the three glacier mass balance parameters (*GLAC_ALB*, *GLAC_ROUGH*
175 and *GLAC_REDF*). The snow related parameters examined are surface roughness (*SNOWROUGH*), albedo of new snow
176 (*NEW_SNOW_ALB*) and albedo decay parameters during the accumulation period (*SNOW_ALB_ACCUM_A*,
177 *SNOW_ALB_ACCUM_B*) and during the thaw period (*SNOW_ALB_THAW_A*, *SNOW_ALB_THAW_B*).

178 The parameters describing snow and glacier properties along with soil and climate parameters are assigned by grid cell. These
179 parameters were initialized with default values and then sampled within prescribed ranges (see Table 3). The same value is
180 assigned to all grid cells within a catchment. The sampling of the soil parameters critical point (*wcr*), wilting point (*wpwp*) and
181 residual moisture (*resid_moist*) is constrained so that conditions required by VIC (Gao et al., 2009) are not violated. Thus,
182 sampling is performed so that $wcr \leq (1 - bd/sdens)$, $wpwp \leq wcr$, and $resid_moist \leq wpwp * (1 - bd/sdens)$.

183 The vegetation parameters consist of the thickness of root zone of the third soil layer (*root_depth*), and the root fractions in all
184 three soil layers. We only sample root fractions in soil layer one and two (*root_fract1*, *root_fract2*) such that the total root
185 fraction in the three soil layers adds to 1. That is, the *root fraction* in soil layer three is updated as $1 - (root_fract1 + root_fract2)$.
186 The vegetation parameters that are considered also include the seasonal leaf area index (*lai*) and seasonal albedo (*albedo*), the
187 architectural resistance (*Rarc*), minimum stomatal resistance (*Rmin*), minimum incoming shortwave radiation at which there
188 will be transpiration (*RGL*), solar attenuation factor (*SolAtm*), wind speed attenuation through the overstory (*WndAtm*) and
189 fraction of the total tree height that is occupied by tree trunks (*Trunk_ratio*). The *lai* parameter governs the amount of water
190 intercepted by the canopy, which controls canopy evaporation. Leaf area index, along with stomatal resistance (*Rmin*), also
191 influences the estimation of vegetation transpiration, and the root fraction dictates the amount of transpiration from each soil
192 layer (Gao et al., 2009). The parameter *Rarc* affects the vertical wind profile.

193 The vegetation parameters are assigned by land cover class. Sampling of these parameters is conducted by adjusting baseline
194 values obtained for each land cover class. The land cover classes were based on the North America Land Cover dataset,
195 edition2 (Natural Resources Canada/The Canada Centre for Mapping and Earth Observation (NRCan/CCMEO) et al. 2013)
196 produced as part of the North America Land Change Monitoring System (NALCMS). In total, 22 land cover classes were
197 identified. For most of these parameters, sampling is conducted by applying a multiplication factor, sampled in the range 0.5
198 to 2.0, to the baseline values. The same sampled parameter is applied to all vegetation classes. To reduce the number of
199 vegetation parameters, a multiplier factor is applied on a seasonal basis for the monthly parameters *LAI* and *albedo*, following
200 a similar approach of Bennett et al., (2018). For example, *lai_dif* is the multiplier factor applied to leaf area index values during
201 winter months (i.e., December, January, and February). The *trunk ratio* is sampled around the defined value by applying an
202 additive change in the range -0.2 to 0.2 so that *trunk ratio* values remain between 0.1 and 0.8. The monthly roughness and
203 displacement height parameters were not sampled. They are specified as a function of vegetation height (which is constant
204 within classes, but variable between classes) and leaf area index as described by Choudhury and Monteith (1988).

205 **2.4 Sensitivity analysis**

206 We applied the Efficient Elementary Effects (EEE) screening method introduced by Cuntz et al. (2015) as a frugal
207 implementation of the Morris method (Morris, 1991). It was developed to identify the model parameters that are most
208 informative regarding a certain model output. The strength of the method lies in it requiring only a small set of model
209 evaluations to separate informative vs. noninformative parameters. On average, EEE requires $10N$ model runs with N being
210 the number of model parameters. EEE does not require algorithmic tuning and converges by itself. The method has been tested
211 for a large range of sensitivity benchmarking functions and a hydrologic model at several locations by Cuntz et al. (2015). The
212 method has further been applied to obtain the informative parameters in complex hydrologic (Cuntz et al., 2016) and land-
213 surface models (Demirel et al., 2018).

214 The EEE approach samples model parameters in trajectories as initially described by Morris (1991) and improved by
 215 Campolongo et al. (2007). A “trajectory” is defined as a sequence of $(N+1)$ parameter sets where the first parameter set is
 216 sampled randomly while all subsequent sets i ($i > 1$) differ from the prior set $(i-1)$ in exactly one parameter value. Such
 217 trajectories allow an efficient sampling of the whole parameter space while considering parameter interactions to a certain
 218 extent. In the approach of Cuntz et al. (2015), only a small number of such trajectories (M_1 ; here $M_1=5$) are sampled in a first
 219 EEE iteration to lower the computational burden. The resulting $(M_1 \times (N + 1))$ model outputs are derived, and the elementary
 220 effects (EEs) are computed for each parameter following Morris (1991). The elementary effect (EE) quantifies the change in
 221 model output $f(p)$ when a parameter p_i is changed by a fraction of this parameter range Δ . The elementary effect of parameter
 222 p_i is calculated as follows:

$$223 \quad EE_i = \frac{f(p_i+\Delta)-f(p_i)}{\Delta} \quad (1)$$

224 The EEs are used to identify the most informative parameters by deriving a threshold that splits the parameters into a set of
 225 N_{ninf} noninformative parameters and a set of $N_{inf}=N-N_{ninf}$ informative parameters. The threshold T is derived automatically
 226 within the EEE method and is based on the EEs of the model outputs provided in the first iteration. The threshold is derived
 227 based on fitting a logistic function to the sorted EEs derived and defining the threshold as the point of largest curvature of the
 228 fitted logistic function. Defining the threshold that is used to separate informative and non-informative parameters in this
 229 approach has been demonstrated using a wide range of test functions and real-world examples, and the reader is referred to
 230 Cuntz et al. (2015) for further details. In the next EEE iteration, a new N -dimensional parameter set is randomly sampled but
 231 this time only the N_{ninf} noninformative parameters are perturbed while the N_{inf} informative parameters are kept at their initially
 232 sampled values. Hence, this trajectory contains only $N_{ninf}+1$ parameter sets. M_2 of such trajectories are sampled in this step
 233 (here $M_2=1$). The derivation of model outputs and the calculation of EEs is repeated. If the EE of any noninformative parameter
 234 exceeds the previously derived threshold T , the previously noninformative parameter will be added to the set of informative
 235 parameters. This EEE iteration (sampling a new trajectory and then adding parameters with an EE above T to the set of
 236 informative parameters) is repeated until no further parameter is reclassified as informative. The final EEE iteration is to
 237 sample M_3 trajectories (here $M_3=5$) to confirm that the set of N_{ninf} noninformative parameters is stable, and no further parameter
 238 is found to be informative. The EEE method parameter values (M_1 , M_2 , and M_3) utilized here are the default settings tested and
 239 recommended by Cuntz et al. (2015). The implementation, documentation, and examples for EEE are open source (Mai and
 240 Cuntz, 2020).

241 **2.5 Transferability of parameter sensitivity**

242 We applied the EEE method to each of the 25 basins and the three model outputs (streamflow, evaporation, snow water
 243 equivalent) independently, leading to 75 sets of noninformative/informative parameters. The initial set of N randomly sampled
 244 model parameter values was the same for all 75 experiments. An average of 430 model runs were required for all 75 EEE
 245 experiments to identify which of the 44 VIC-GL parameters analyzed in this study were informative.

246 Informative and noninformative parameters were compared over the 25 basins to identify parameters that are informative
 247 across all basins (termed invariant-informative parameters), 2) parameters that are non-informative across all basins (invariant-
 248 noninformative, and 3) parameters that are informative in some basins but not others (variant-informative).

249 We evaluated the potential of using watershed classification as a tool to transfer parameter SA information. Climatic conditions
 250 exert a major control on runoff generation (Yadav et al., 2007; Sawicz et al., 2011) and have been found to have a higher
 251 impact on parameter sensitivity than vegetation and soil conditions (Rosero et al., 2010). However, vegetation and soil
 252 conditions can affect other hydrologic quantities. For example, Bennett et al. (2018) found that canopy spacing plays an
 253 important role in snow water equivalent simulation by VIC. Here, we used aridity index, snow index and the percentage of
 254 glacier area, and the percentage of area covered by each of several vegetation classes to classify the 25 basins. Although 22
 255 vegetation classes are defined for VIC-GL, we only considered the four vegetation classes listed in Table 4 that are dominant
 256 in the study area. To evaluate the impact of vegetation on informative parameter identification, watershed classification was
 257 first performed using the climatic attributes only, and then by combining climatic and vegetation class cover attributes.

258

259 **Table 4: Statistics of the percentage of VIC land cover classes (%) identified using NALCMS and considered in this study over the**
 260 **25 selected basins.**

Class ID	Description	Min	Max	Mean
2	Temperate or sub-polar needleleaf forest - high-elevation	0.1	46	18
4	Temperate or sub-polar needleleaf forest - coastal/humid/dense	0	29	9
9	Mixed Forest	0	34	4
11	Temperate or sub-polar shrubland	0.4	91	19

261 To classify the 25 basins into homogenous groups, the agglomerative hierarchical algorithm was used with the Euclidean
 262 distance and Ward's criterion (Roux, 2018). Agglomerative hierarchical clustering consists of a series of successive fusion of
 263 watersheds into groups according to their similarity. It starts by considering each element x (i.e., watershed) as a cluster $\{x\}$
 264 then continue by creating new cluster by merging the two closest clusters. The dendrogram, a tree diagram, illustrates the
 265 merging process of the agglomerative hierarchical clustering. The Ward method used here aggregates clusters so that within-
 266 group inertia (i.e. multidimensional variance) is minimal.

267 To test our hypothesis that parameter sensitivity can be generalized using watershed classification we conducted the following
 268 evaluation. Each sub-basin was set as the target basin. For each target basin, informative parameters are transferred using a
 269 number of donor basins of the same cluster. Using multiple donor basins has been shown to provide better results than a single
 270 donor basin (e.g. Oudin et al., 2008; Bao et al., 2012). Let A be a target basin of cluster C_i . We assume that informative
 271 parameters of basin A are the intersection of informative parameters of x donor basins from cluster C_i . For each target basin

272 A, informative parameters are transferred using all possible combinations of x donor basins of cluster C_i not including A. This
273 test aims at evaluating whether x donor basins could be used to generalize informative parameters for each cluster.
274 The performance of watershed classification to identify informative and noninformative parameters in a basin is evaluated
275 using the $F1$ score. This score is often used to measure the performance of a binary classification (Chicco and Jurman, 2020).
276 The $F1$ score is a weighted average of precision and recall. Assuming two classes, positive (informative) and negative
277 (noninformative), the $F1$ score measures the ability to correctly and incorrectly predict the two classes. Considering counts of
278 TP true positive (i.e., informative predicted as informative), FP false positive (informative predicted as noninformative), and
279 FN false negative (noninformative predicted as informative), we can obtain measures of precision, recall and the $F1$ score as
280 follows:

$$281 \text{ Precision} = \frac{TP}{TP+FP}, \quad (2)$$

$$282 \text{ Recall} = \frac{TP}{TP+FN}, \quad (3)$$

$$283 \text{ F1 score} = 2 * \frac{\text{Precision} \times \text{Recall}}{\text{Precision} + \text{Recall}} \quad (4)$$

284

285 The $F1$ score takes values between 0 and 1, where 0 means that all positive (here informative parameters) are predicted as
286 negative (i.e., as noninformative) and 1 means perfect classification with $FN=FP=0$.

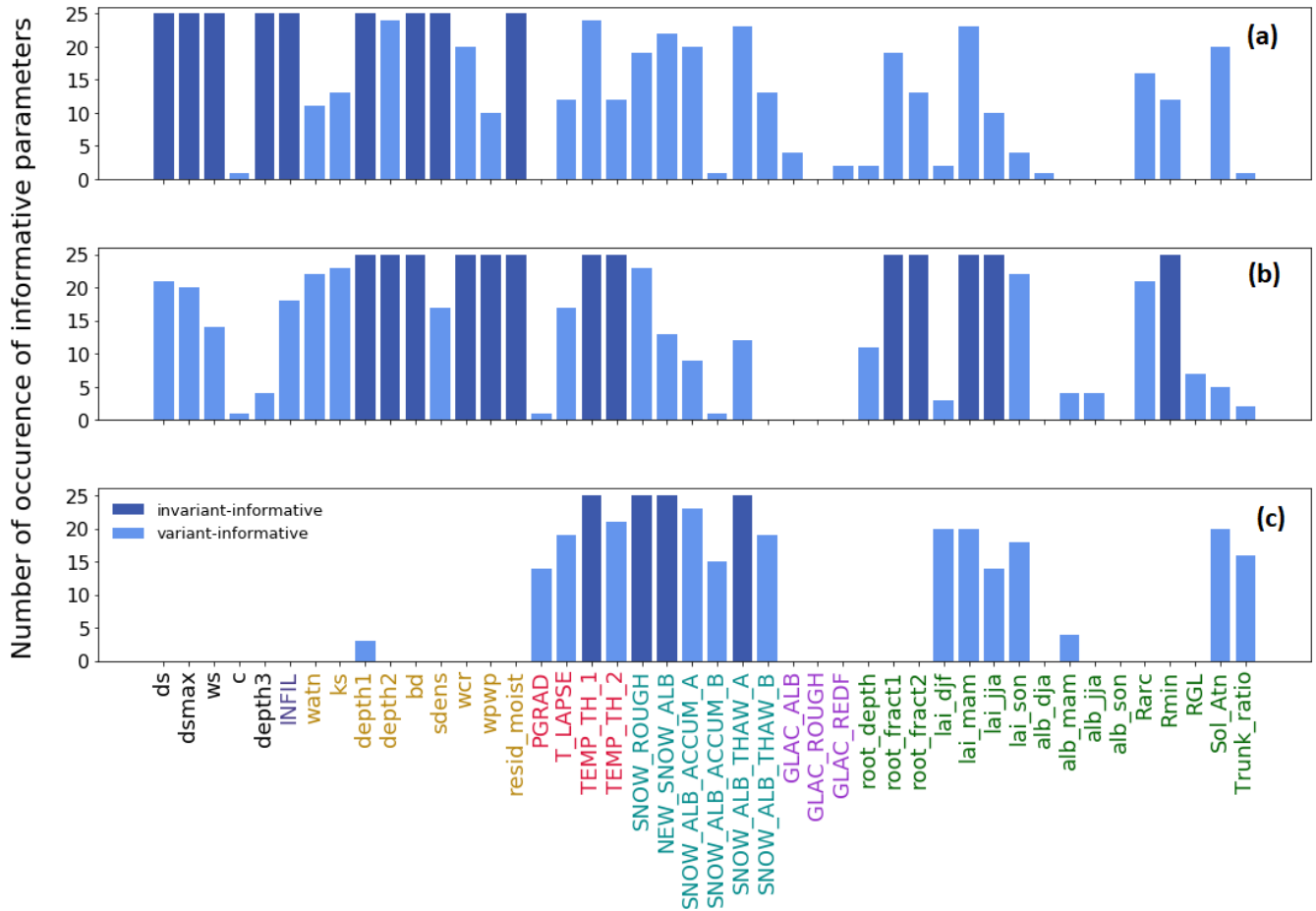
287 For a given number of donor basins x , the $F1$ score is reported for each target basin A as the average $F1$ score calculated
288 between sensitive parameters of A and identified sensitive parameters from all possible combinations of the x donor basins.
289 This is done for each classification method, climate-based and climate-land cover-based clustering, to evaluate performance
290 in identifying sensitive parameters by watershed groupings provided by each clustering analysis. Then, we use the Wilcoxon
291 signed rank test to compare the $F1$ scores for the 25 basins obtained using the two clustering methods so that we can determine
292 whether incorporating land cover in watershed classification improves the ability to predict informative parameters. The
293 Wilcoxon signed rank test tests the null hypothesis that the $F1$ score resulting from both clustering analyses are from the same
294 distribution i.e., have similar ability to identify informative parameters.

295 **3 Results**

296 The sensitivity analysis using the EEE method was performed with respect to three model outputs independently: streamflow,
297 evapotranspiration, and snow water equivalent. Figure 2 presents the number of occurrences of informative parameters over
298 the 25 selected sub-basins for the three outputs. From this figure, we can identify the three parameter categories, invariant-
299 informative, invariant noninformative and variant-informative for each hydrologic process. Table 5 summarizes the three
300 parameter categories per model output. Amongst the 44 VIC-GL parameters only 9 parameters are invariant-informative for
301 streamflow, 13 are invariant-informative for evapotranspiration and 4 are invariant-informative for snow water equivalent. A

302 large percentage of parameters are variant-informative for these fluxes with 29 parameters for streamflow, 25 parameters for
 303 evapotranspiration and 14 parameters for snow water equivalent. We first examine the sensitive parameters and their spatial
 304 variability per model output in Sect. 3.1 to 3.3. We further analyze the performance of the physical similarity approach for
 305 transferring sensitivity analysis information and the attributes that are informative for each model output (Sect. 3.4).

306



307
 308 **Figure 2: Number of occurrences of informative parameters for streamflow (a), evapotranspiration (b) and snow water equivalent**
 309 **(c) over the 25 studied sub-basins. Parameters are considered invariant-informative if the count of basins in which they are**
 310 **informative equals 25, invariant-noninformative if that count is 0, and variant-informative if the count is between 1 and 24.**

311

312 **Table 5: VIC-GL parameter importance regarding streamflow, evapotranspiration (ET) and snow water equivalent (SWE).**

Process	Invariant-informative parameters	Invariant-noninformative parameters	Variante-informative parameters
Streamflow	ds, dsmax, ws, depth3, INFIL, depth1, bd, sdens, resid_moist	PGRAD, GLAC_ROUGH, alb_mam, alb_jja, alb_son, RGL	c, T_LAPSE, watn, ks, depth2, wcr, wpwp, SNOW_ROUGH, NEW_SNOW_ALB, SNOW_ALB_ACCUM_A, SNOW_ALB_ACCUM_B, SNOW_ALB_THAW_A, SNOW_ALB_THAW_B, TEMP_TH_1, TEMP_TH_2, GLAC_ALB, GLAC_REDF, root_depth, root_fract1, root_fract2, lai_djf, lai_mam, lai_jja, lai_son, alb_dja, Rarc, Rmin, Sol_Atn, Trunk_ratio
ET	depth1, depth2, bd, wcr, wpwp, resid_moist, TEMP_TH1, TEMP_TH2, root_fract1, root_fract2, lai_mam, lai_jja, Rmin	SNOW_ALB_THAW_B, GLAC_ALB, GLAC_ROUGH, GLAC_REDF, alb_dja, alb_son	ds, dsmax, ws, c, depth3, INFIL, PGRAD, T_LAPSE, watn, ks, sdens, SNOW_ROUGH, NEW_SNOW_ALB, SNOW_ALB_ACCUM_A, SNOW_ALB_ACCUM_B, SNOW_ALB_THAW_A, root_depth, lai_djf, lai_son, alb_mam, alb_jja, Rarc, RGL, Sol_Atn, Trunk_ratio
SWE	SNOW_ROUGH, NEW_SNOW_ALB, SNOW_ALB_THAW_A, TEMP_TH1	ds, dsmax, ws, c, depth3, INFIL, watn, ks, depth2, bd, sdens, wcr, wpwp, resid_moist, GLAC_ALB, GLAC_ROUGH, GLAC_REDF, root_depth, root_fract1, root_fract2, alb_dja, alb_jja, alb_son, Rarc, Rmin, RGL,	PGRAD, T_LAPSE, depth1, SNOW_ALB_ACCUM_A, SNOW_ALB_ACCUM_B, SNOW_ALB_THAW_B, TEMP_TH_2, lai_djf, lai_mam, lai_jja, lai_son, alb_mam, Sol_Atn, Trunk_ratio

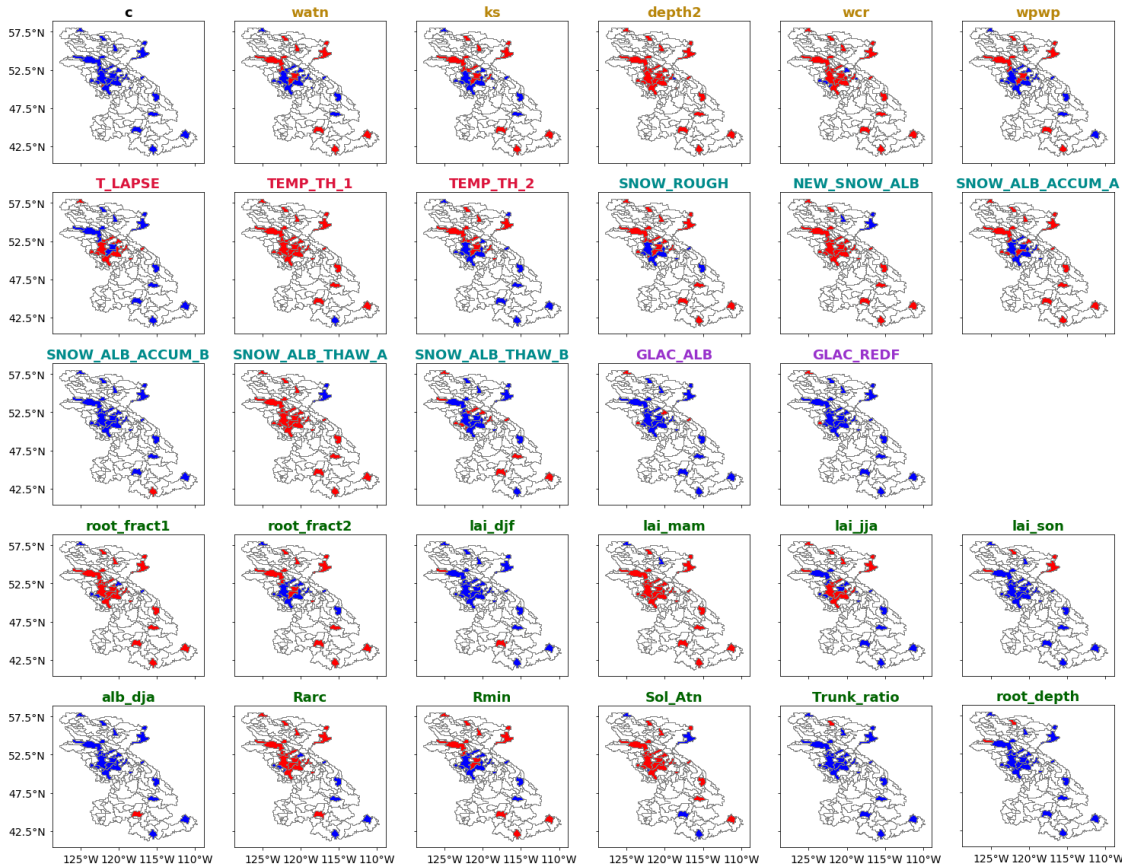
313

314 3.1 Informative parameters for streamflow

315 The soil parameters *ds*, *dsmax*, *ws*, *depth3*, *depth1* are consistently identified as sensitive to streamflow (e.g., Demaria et al.,
316 2007; Bennett et al., 2018; Gou et al., 2020) and this reflects the empirical nature of the runoff and baseflow processes that are
317 fundamental in the VIC family of models. In addition to these parameters, the soil parameters soil bulk density (*bd*), soil
318 particle density (*sdens*) and the residual moisture (*resid_moist*) are also identified as invariant-informative to streamflow in
319 the study area.

320 Figure 3 presents the sensitivity of the 29 variant-sensitive parameters with respect to streamflow (Table 5). These parameters
321 include the remaining soil parameters, climate, snow, and most of the vegetation parameters. The climate parameters
322 *TEMP_TH_1* and *TEMP_TH_2* (i.e., the rain/snow temperature threshold parameter 1 and 2) have different sensitivity
323 patterns. The parameter *TEMP_TH_1* is found to be informative across all basins except in the arid basin BruneauR, which
324 has the lowest snow index (0.38). The parameter *TEMP_TH_2* is informative only in sub-basins located in the interiors of the
325 Fraser and Peace. *T_LAPSE* is informative in the snow-dominated basins of the Fraser and the Columbia. The snow-related

326 parameters show different spatial sensitivity. For instance, *SNOW_ROUGH* is sensitive over all basins except for some snow-
 327 dominated basins of the Fraser and Columbia. The *NEW_SNOW_ALB* and *SNOW_ALB_THAW_A*, which control snow melt,
 328 are sensitive across all basins except the semi-arid basins of the Peace (north-east of the study region). Snowmelt in the study
 329 area contributes significantly to runoff, which explains the sensitivity of these parameters for streamflow. These results are
 330 consistent with the results found by Houle et al. (2017) who evaluated sensitivity of these parameters to snow water equivalent
 331 using the Sobol' method (Sobol', 1990).



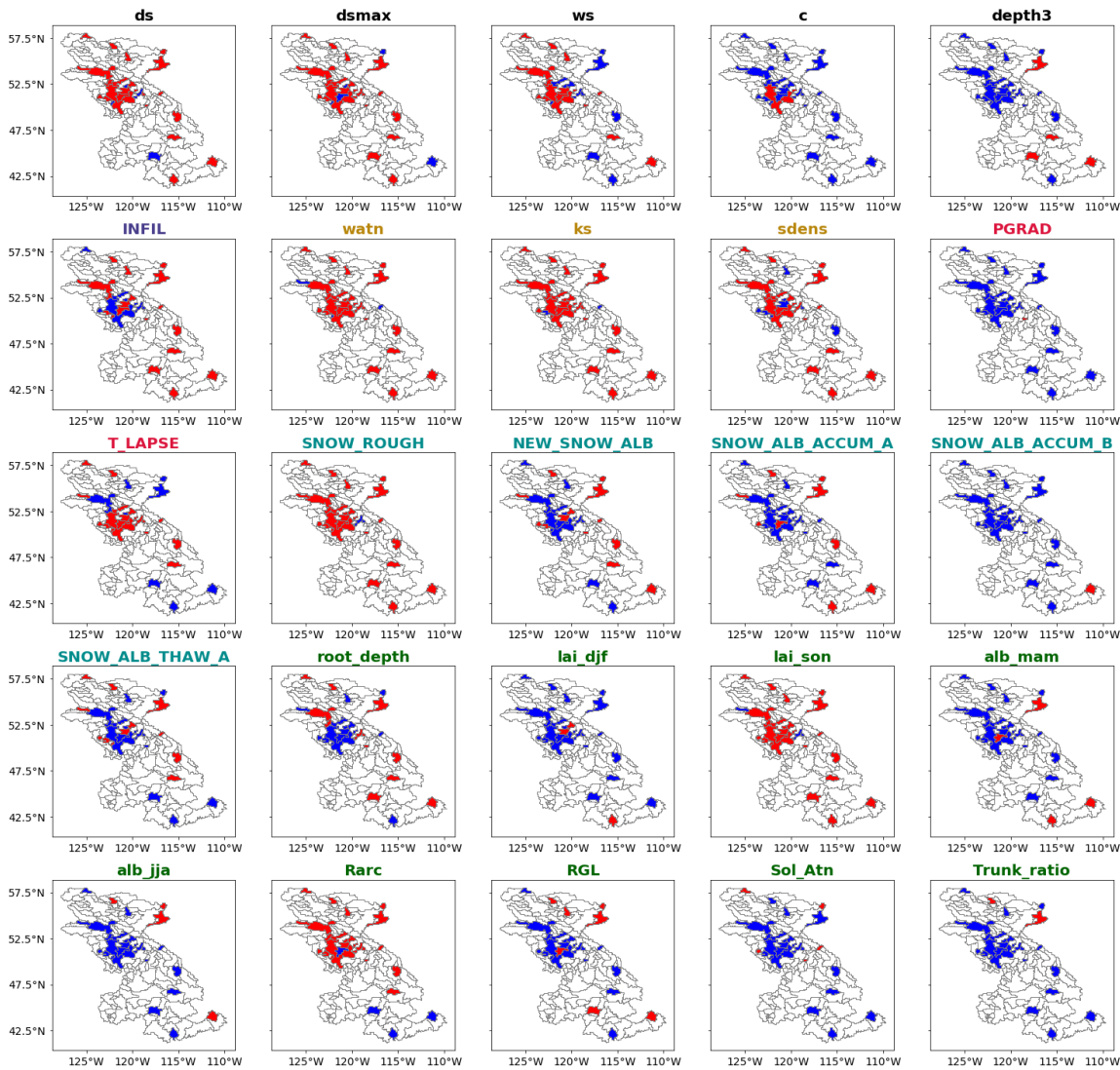
332
 333 **Figure 3: The spatial sensitivity of the 29 streamflow variant-informative parameters with red being informative and blue non-**
 334 **informative over the 25 selected basins. The nine invariant informative and six invariant non-informative parameters are not**
 335 **included.**

336 In the semi-arid and arid basins, the exponent in Campbell's equation for hydraulic conductivity (*watn*), the saturated
 337 hydrologic conductivity (*ks*), and fractional soil moisture content at the wilting point (*wpwp*) are informative for streamflow.
 338 The *wpwp* parameter dictates baseflow estimation with the Arno model formulation (Francini and Pacciani, 1991) used in VIC
 339 (Gao et al., 2009). Given the limited precipitation in these basins, baseflow may be a significant streamflow source that explains
 340 the importance of this parameter in these basins. The root depth of the third layer (*root_depth*) is sensitive in the northern semi-

341 arid basins (NAUTL, HRNFC). The root fraction of the first layer (*root_fract1*) is sensitive in Columbia basins and the non-
342 glacierized basins of the Fraser and Peace. The root fraction in the second layer (*root_fract2*) is sensitive only in the semi-arid
343 and arid basins. The sensitivity of the LAI parameters is seasonal with springtime LAI being sensitive in almost all basins.
344 For the glacierized headwater catchments the albedo of the glacier surface (*GLAC_ALB*) is informative for streamflow. The
345 importance of this parameter increases with the basin glacier area and this parameter is influential in the four basins CLEAO,
346 KWRNW, DONAL, and TASEK with the largest glacier area (between 115 km² and 194 km², between 7 % and 11 % of
347 watershed area). The remaining glacierized basins have much smaller glacier areas (less than 1.5 % of the watershed area).
348 The *GLAC_REDF* parameter is informative for streamflow as well in the western-glaciated basins TASEK and KWRNW,
349 where average annual temperature is negative. Glaciers behave as natural water reservoirs that provide streamflow through ice
350 melt and temporary meltwater storage within the glacier during late summer (Marshall et al., 2011). For instance, in the upper
351 Columbia, glaciers contribute up to 25 % and 35 % of streamflow in August and September respectively and up to 6 % to the
352 annual streamflow (Jost et al 2012, Jiskoot and Muller, 2012).

353 **3.2 Informative parameters for evapotranspiration**

354 There are 13 invariant-informative parameters that affect evapotranspiration in the study region (see Fig. 2 and Table 5). These
355 include parameters that control soil drainage (*wcr*, *wpwp*, *resid_moist*), and soil storage capacity (*bd*, *depth1* and *depth2*). The
356 invariant-informative parameters also include the climate parameters *TEMP_TH_1*, *TEMP_TH_2* and vegetation parameters
357 seasonal leaf area index (*lai_mam*, *lai_jja*), minimum stomatal resistance (*Rmin*), and root fraction (*root_fract1*, *root_fract2*).
358 The VIC-GL model computes evapotranspiration as the sum of four types of evaporation; evaporation from the canopy layer,
359 transpiration from all three soil layers, soil evaporation from the top soil layer, and evaporation/sublimation from the snow or
360 glacier surface (Liang et al., 1994). The soil parameters affect the bare soil evaporation that occurs at the top thin layer. The
361 leaf area index parameters govern the amount of water intercepted by the canopy, which controls canopy evaporation. Leaf
362 area index and stomatal resistance (*Rmin*) influence the estimation of vegetation transpiration and the root fraction dictates the
363 amount of transpiration from each soil layer (Gao et al., 2009). These parameters are defined for each land cover type in the
364 vegetation library. They are typically fixed based on observed values, which ignores the large estimation and scaling
365 uncertainties around their values (Mendoza et al., 2015). In this paper, the sampling of *LAI* and *Rmin* values is based on a
366 perturbation of observed values (see Table 3; Type “Multiplicative factor”). The sensitivity of evapotranspiration to this
367 perturbation illustrates the need to obtain accurate values for these parameters or consider their uncertainty in the model
368 calibration process. The rain/snow temperature thresholds (*TEMP_TH_1*, *TEMP_TH_2*) are likely to impact the throughfall
369 (water that penetrates a plant canopy) and rainfall/snow interception (rain captured, stored, and evaporated from the vegetation
370 surface) (Levia et al., 2019).



371

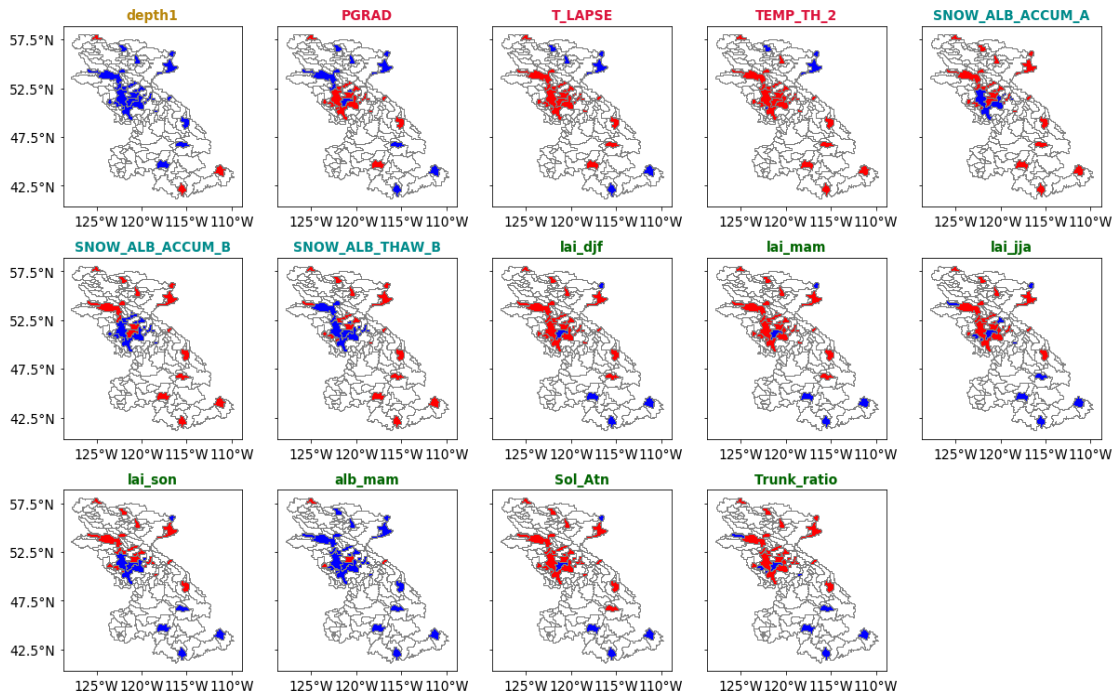
372 **Figure 4: The spatial sensitivity of the 25 evapotranspiration variant-informative parameters with red being informative and blue**
 373 **non-informative over the 25 selected basins. The 13 invariant informative and 6 invariant non-informative parameters are not**
 374 **included. For the number of occurrences of informative parameters see Figure 2.**

375 Table 5 lists the six invariant-noninformative parameters for evapotranspiration which are the glacier parameters, autumn and
 376 winter vegetation albedo, and the albedo decay exponent during the thaw period *SNOW_ALB_THAW_B*. Figure 4 presents the
 377 spatial sensitivity of the 25 variant-informative parameters with respect to evapotranspiration. Some parameters show a clear
 378 spatial pattern of sensitivity that is related to basin physical characteristics. For instance, *T_LAPSE* is sensitive in snow-
 379 dominated basins, whereas *INFIL* and *sdens* are sensitive in semi-arid and arid basins. The baseflow parameters (*ds*, *dsmax*)
 380 are informative in most basins while the parameter *ws* is only informative in humid sub-basins. The surface roughness of the

381 snowpack (*SNOW_ROUGH*), the architectural resistance of vegetation (*Rarc*), which affects the vertical wind profile, and
382 autumn leaf area index (*lai_son*) are also influential to evapotranspiration in most basins.

383 **3.3 Informative parameters for snow water equivalent**

384 Amongst the six snow-parameters, only three (*SNOW_ROUGH*, *NEW_SNOW_ALB*, *SNOW_ALB_THAW_A*) are invariant-
385 informative for snow water equivalent. The climate parameter *TEMP_TH_1* is also invariant-informative for snow water
386 equivalent. The parameter *TEMP_TH_2* is informative in the majority of the basins except in the semi-arid basins of the Peace.
387 The sensitivity of the remaining three snow parameters (*SNOW_ALB_ACCUM_A*, *SNOW_ALB_ACCUM_B*, and
388 *SNOW_ALB_THAW_B*) and the two climate parameters (*PGRAD*, *T_LAPSE*) varies within the study region. Figure 5 presents
389 the sensitivity of the 14 variant-informative parameters for snow water equivalent. The *T_LAPSE* and *PGRAD* are sensitive in
390 the high-altitude basins. The parameter *SNOW_ALB_ACCUM_B* is informative in the basins of the Columbia and Peace, and
391 in the semi-arid basins of the Fraser. The sensitivities of seasonal leaf area index (*lai_djf*, *lai_mam*, *lai_jja*, and *lai_son*), ratio
392 of total tree height that is trunk (*Trunk_ratio*), and the solar attenuation factor (*Sol_Atn*) show a clear spatial pattern. These
393 parameters are informative in basins where forest is the dominant land cover (i.e., Fraser and Peace). The springtime vegetation
394 albedo (*alb_mam*) is sensitive over the snow-dominated basins. The sensitivity of snow water equivalent for vegetation
395 parameters can be explained by the impact of forest cover on snow accumulation and ablation processes, mainly by snowfall
396 interception and modification of incoming radiation and wind speed below the forest canopy (Andreadis et al., 2009). These
397 findings are consistent with those of Houle et al., (2017) and Bennett et al., (2018).



398

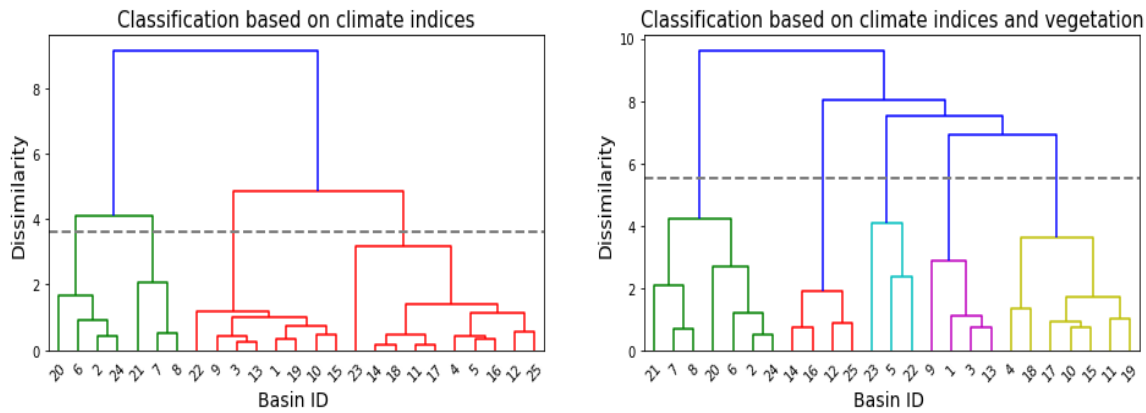
399 **Figure 5: The spatial sensitivity of the 14 snow water equivalent variant-informative parameters with red being informative and blue**
 400 **non-informative over the 25 selected basins. The 4 invariant informative and 26 invariant non-informative parameters are not**
 401 **included. For the number of occurrences of informative parameters see Figure 2.**

402

403 3.4 Watershed classification

404 Figure 6 presents the dendrogram, a diagram tree of clusters resulting from the agglomerative hierarchical clustering using
 405 climate indices and the combination of climate indices and vegetation class cover. Clustering based on climate indices yields
 406 four clusters whereas clustering based on climate indices and vegetation cover results in five clusters.

407

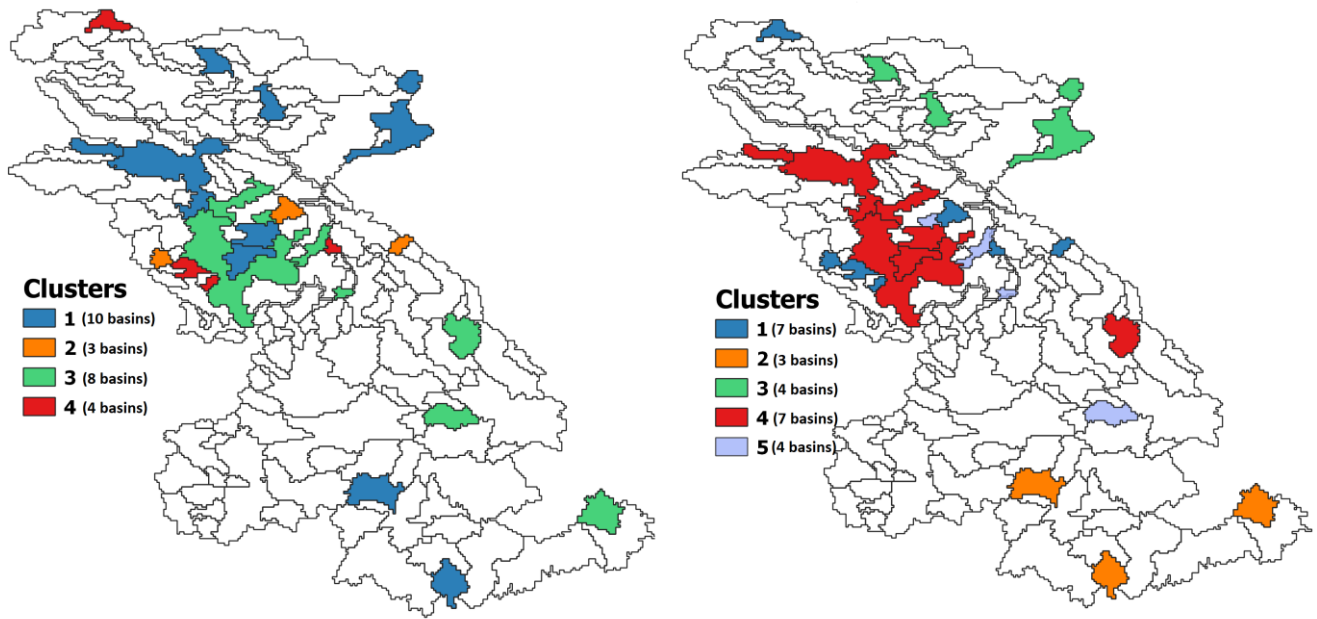


408

409 **Figure 6: Watershed classification dendrogram using climate indices and the combination of climate and vegetation indices. The**
 410 **height of each node represents the distance between its branches and the dashed line represents the cutoff threshold to distinguish**
 411 **the 4 clusters in the case of climate-based classification and 5 clusters in the case of climate-land cover-based classification. The**
 412 **threshold is chosen as a trade-off between cluster dissimilarity and within cluster variance.**

413

414 Figure 7 shows the results of the hierarchical clustering analyses and Fig. 8 and 9 present the attribute statistics for each cluster.
 415 The clusters produced using climatic attributes can be described as follows. Cluster #1 consists of dry basins located in the
 416 southern Columbia, eastern Peace, and central Fraser basins. Cluster #2 contains glacierized watersheds along the Coast
 417 Mountains and the Rocky Mountains. Cluster #3 contains semi-arid basins in the interior Fraser and eastern Columbia, and
 418 cluster #4 contains snow-dominated basins with very low glacier area (less than 4 % of watershed area) compared to cluster
 419 #2. Clusters obtained using both climatic and vegetation attributes correspond to clusters based on climate that were merged
 420 or divided based on vegetation class cover dominance. Cluster #1 contains all glacierized watersheds and corresponds to clusters
 421 #2 and #4 obtained with climatic based clustering. Cluster #2 consist of dry basins dominated by land cover 11 (temperate or
 422 sub-polar shrubland) that are located in the southern Columbia basin. Cluster #3 consist of dry basins dominated by land cover
 423 9 (i.e., mixed forest) located in the eastern Peace River basin. Cluster #4 represents arid basins in the interior Fraser and upper
 424 Columbia dominated by land cover 2 (i.e., temperate or sub-polar needleleaf forest - high-elevation) and cluster #5 consists of
 425 wet basins dominated with land cover 4 (i.e., temperate or sub-polar needleleaf forest - coastal/humid/dense).



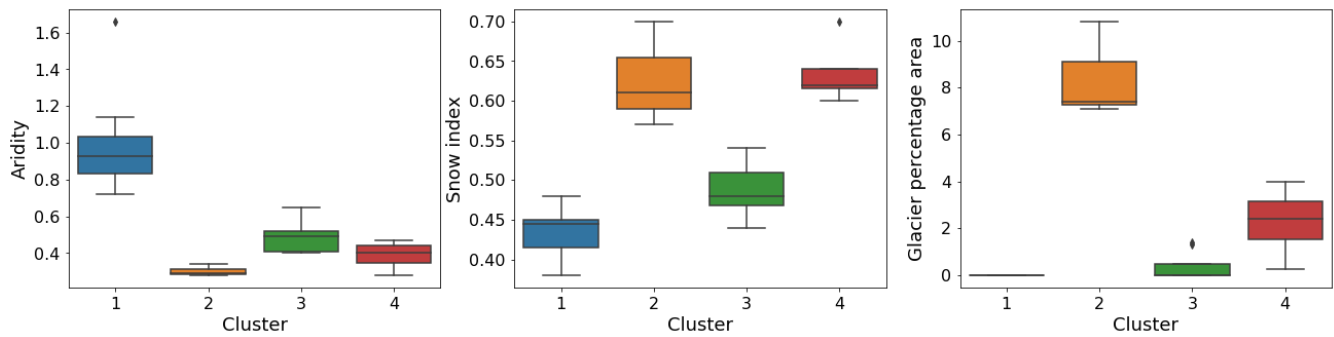
426

427 **Figure 7: Map of clusters obtained using only climatic attributes (left), and using both vegetation- and climatic attributes (right).**

428

429

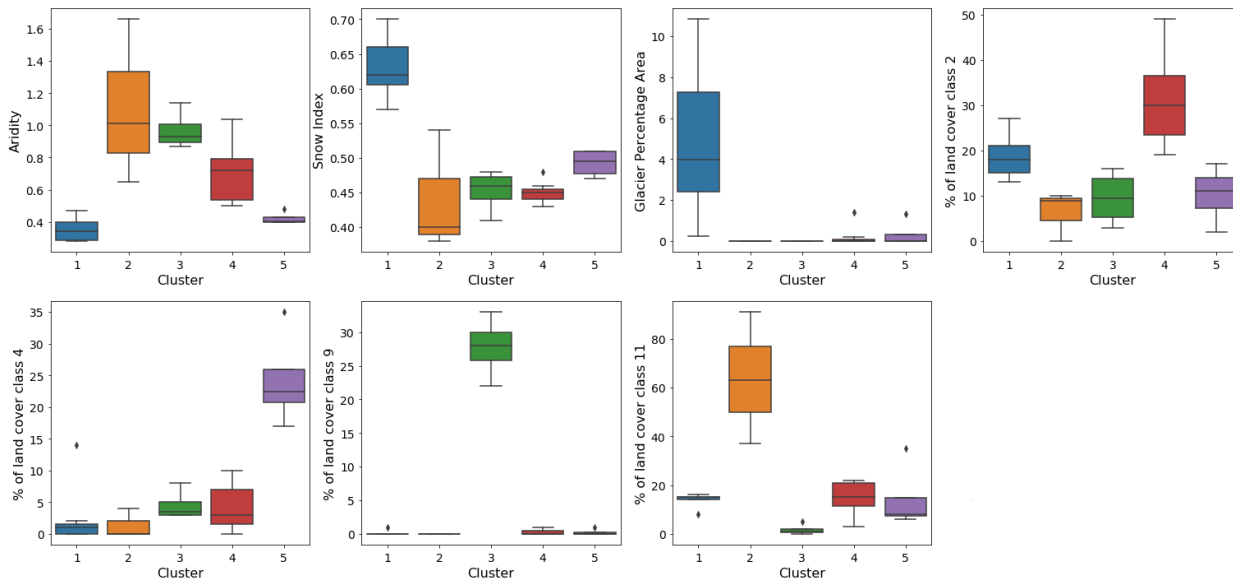
430



431

432 **Figure 8: Box-plots of the climate attributes for each cluster produced by climate based classification.**

433



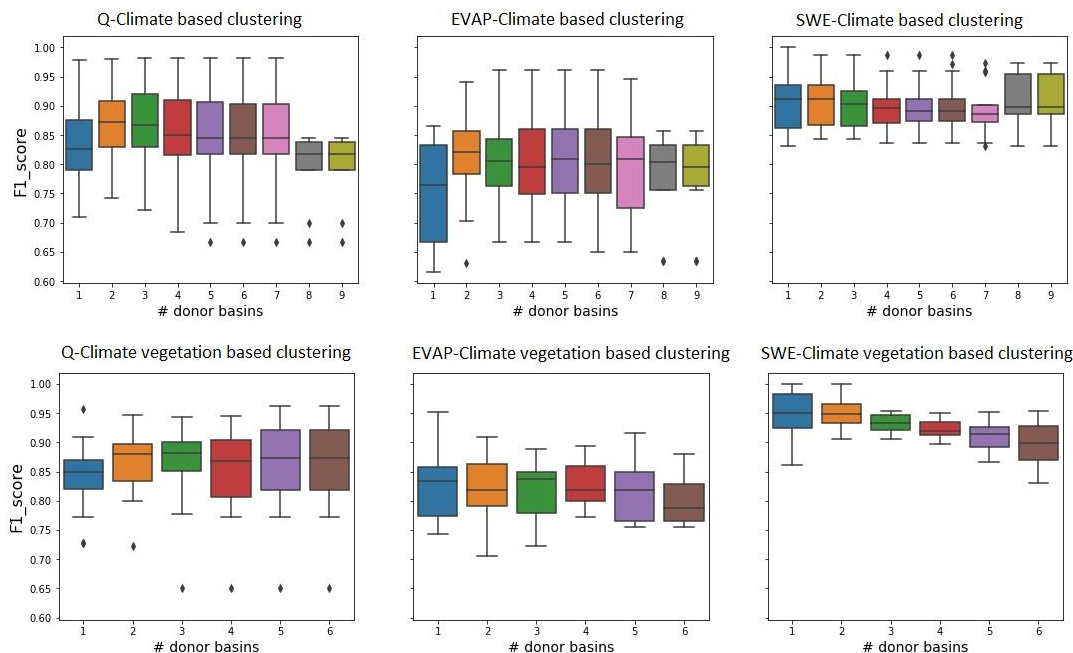
434

435 **Figure 9: Box-plots of attributes of each cluster produced by climate- and vegetation-based classification.**

436

437 **3.5 Watershed classification as a way to transfer parameter sensitivity**

438 The distribution of *FI* scores obtained by transferring informative parameters for streamflow, evaporation and snow water
 439 equivalent using both clustering analyses and a range of donor basins is presented in Fig. 10. The *FI* scores calculated for
 440 transferring streamflow informative parameters based on climatic attributes range between 0.66 (using 9 donor basins) and
 441 0.98 (using between three to seven donor basins), whereas this score ranges between 0.65 (using six donor basins) and 0.96
 442 (using six donor basins) when using both climate and vegetation attributes. For evapotranspiration the *FI* scores obtained by
 443 climatic based clustering range between 0.63 (using six donor basins) and 0.96 (using three to six donor basins). The scores
 444 range between 0.7 (using two donor basins) and 0.95 (using a single donor basin) when using both climatic and land cover
 445 attributes for clustering analysis. The *FI* scores for snow water equivalent range between 0.83 (using four to nine donor basins)
 446 and 1 (using one to two donor basins) when transferring informative parameters based on climatic attributes and the
 447 combination of climatic attributes and vegetation.



448

449 **Figure 10: *F1* score distribution obtained by transferring informative parameters over the 25 basins.**

450

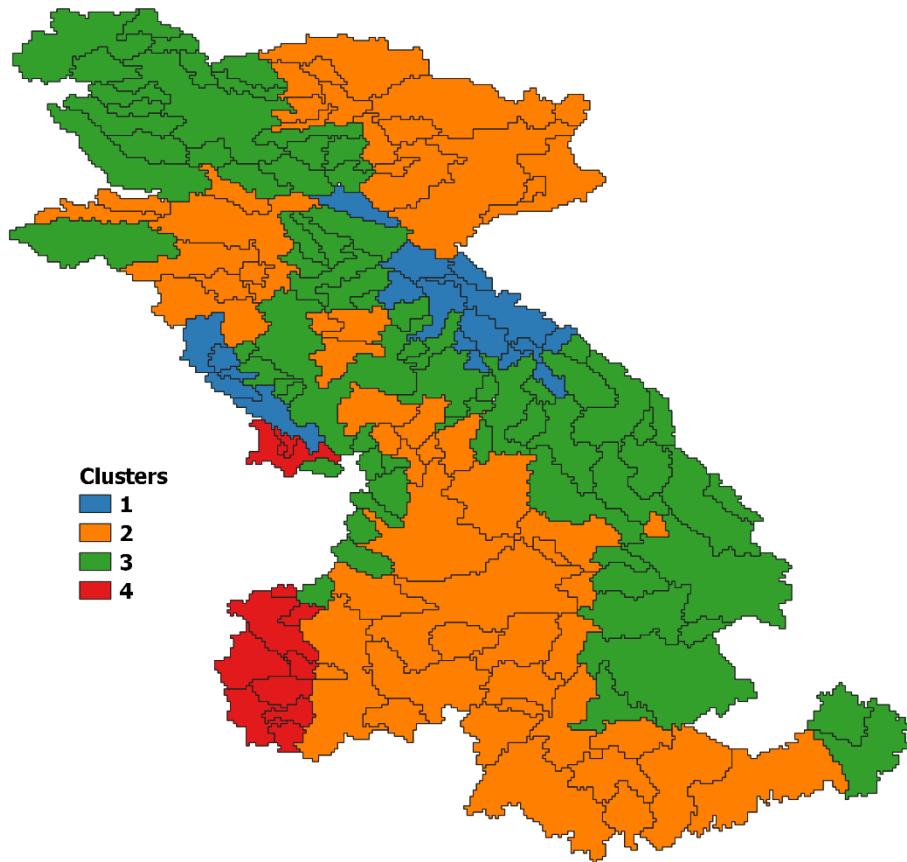
451 Transferring informative parameters based on more than a single donor basin improves the *F1* score except when transferring
 452 evapotranspiration informative parameters using climatic and vegetation clustering analysis. Overall, the results shows that
 453 two donor basins would be sufficient to generalize informative parameters to each cluster. Therefore, for each model output
 454 we compare the *F1* distributions using two donor basins based on both clustering analysis with the Wilcoxon test. The p-value
 455 of the test applied to *F1* score distributions obtained by transferring streamflow informative parameters is 0.49 and by
 456 transferring evapotranspiration informative parameters is 0.48. Hence, the *F1* score distributions using climatic clustering
 457 analysis and climatic-land cover analysis are not significantly different. Therefore, using only climatic attributes would be
 458 sufficient to transfer informative parameters to streamflow and evapotranspiration. These findings are consistent with other
 459 VIC studies (Demaria et al., 2007) and for other hydrologic models (e.g., Rosero et al., 2010) showing that parameter sensitivity
 460 for streamflow can be transferred based predominantly on climate similarity.

461 The Wilcoxon test statistic applied to the *F1* distribution resulting from transferring snow water equivalent informative
 462 parameters is 31 with a p-value of 0.0006. This suggests that there is a significant improvement when using both climatic and
 463 land cover attributes to transfer snow water equivalent parameter sensitivity. The importance of land cover and vegetation
 464 properties as a control on snow accumulation and ablation is consistent with previous studies (e.g., Bennett et al., 2018).

465 4 Discussion

466 In this work, we have examined the sensitivity of an extensive list of VIC parameters to streamflow, evapotranspiration, and
467 snow water equivalent over 25 basins spanning a range of hydroclimatic conditions. We found that informative parameters
468 vary spatially with climate and land cover depending on the model output considered. The findings are in line with previous
469 VIC sensitivity analysis studies (e.g., Demaria et al., 2007; Bennett et al., 2018; Gou et al., 2020, Sepúlveda, 2021). In addition,
470 the two climate parameters temperature lapse rate (T_LAPSE) and the precipitation gradient ($PGRAD$) omitted in previous
471 studies have been found to be informative to headwater glacierized watersheds and snow dominated non-glacierized
472 watersheds. The T_LAPSE parameter is typically fixed when developing gridded meteorological data. For instance, Bohn et
473 al., (2016) used a gridded temperature corrected with a lapse rate of 6.5 °K/km to force VIC over southwestern US and
474 northwestern Mexico. However, several studies have indicated that the often-used constant lapse rates 6-6.5 °C/km are not
475 representative of the surface conditions over different mountainous regions and may differ for each slope within the same
476 mountain (Blandford et al., 2008; Minder et al., 2010, Córdova et al., 2016).

477 In this study, we showed that watershed classification helps identify spatial patterns of informative parameters at a reduced
478 cost. Hence, it reduces the cost of performing sensitivity analysis at the same scale of large-scale land surface models. In our
479 case, watershed classification based on climatic attributes (snow and aridity index) and percentage of glacier area was sufficient
480 to transfer parameter sensitivity between basins of similar attributes. However, incorporating vegetation class cover
481 significantly improved the identification of sensitive parameters for snow water equivalent. The results show that two donor
482 basins per cluster are sufficient to identify sensitive parameters. These results imply that the cost of running sensitivity analysis
483 over a large domain encompassing N clusters of basins would be reduced to the cost of running 2N sensitivity analyses. The
484 information gained can then be extrapolated to large domain based on sub-watershed membership to the N clusters. Thus,
485 candidate parameters for model calibration can be identified at a substantially reduced computational cost as compared to
486 running a large-domain sensitivity analysis. For example, climatic based classification of the 158 basins that covers the entire
487 domain results in four watershed clusters (see Fig. 11) as follows. Cluster #1 consist of glacierized basins along the Coast
488 Mountains and Rocky Mountains. Cluster #2 groups dry basins located in interior and southern Columbia, eastern Peace, and
489 upper Fraser basins. Cluster #3 contains snow-dominated basins in north Peace River basin and eastern Columbia River basin
490 whereas Cluster #4 contains rainfall dominated basins in western Columbia River basin. These clusters are consistent with the
491 clusters obtained by classifying the 25 basins except for cluster #4 because the sample of the studied basins does not include
492 any rainfall-dominated basins. Hence, the cost of performing a sensitivity analysis across the 158 basins is reduced to the cost
493 of evaluating parameter sensitivity over eight basins (i.e., two basins for each basin cluster).



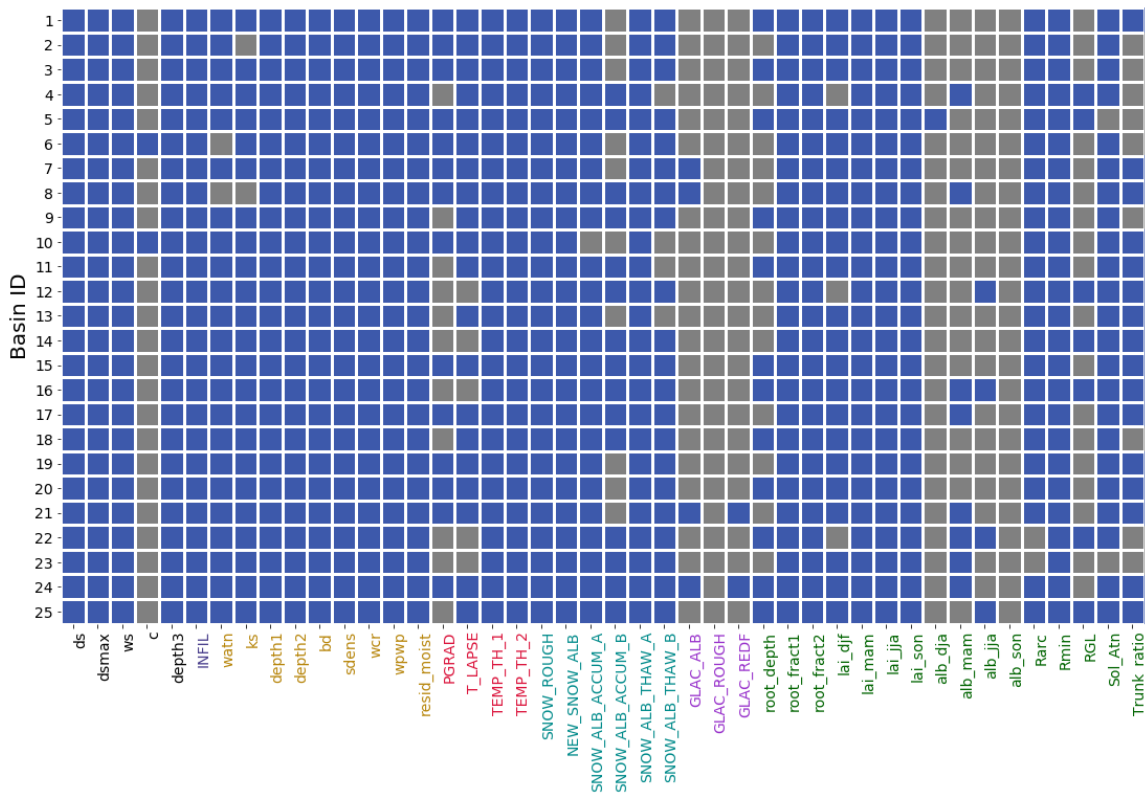
494

495 **Figure 11: Climatic based classification of the 158 sub-basins of the Peace River, Fraser River, and Columbia River basins.**

496

497 It has been argued in the literature that calibration based solely on streamflow is not sufficient to ensure model accuracy and
 498 fidelity (Rakovec et al., 2016). To improve model realism, recent calibration strategies follow a process-based approach. This
 499 approach relies either on adjusting model parameters against hydrological signatures extracted from streamflow timeseries that
 500 link to the underlying model processes (Yilmaz et al., 2008; Euser et al., 2013, Shafii and Tolson; 2015; Rakovec et al., 2016),
 501 against measurements of different model outputs such as evapotranspiration, snow cover, and baseflow (e.g., Isenstein et al.,
 502 2015, Ismail et al., 2020), or by hydrograph decomposition (e.g., He et al., 2015, Shafii et al., 2017; Larabi et al., 2018).
 503 However, we recognize that the effort to constrain multiple hydrologic processes will require a substantial increase in the size
 504 of the parameter domain during model calibration. For instance, our sensitivity analysis results from Table 5 and Fig. 12
 505 suggest that calibrating VIC-GL in a multi-objective/multi-variable framework would require a high number of parameters in
 506 the calibration process (30 to 38 parameters depending on the sub-basin if one is to consider all informative parameters for
 507 each output considered here). Across the 25 sub-basins, an average of 77 % of parameters (34 of 44 parameters analyzed) are

508 informative to at least one of simulated streamflow, evapotranspiration, or snow water equivalent (see Fig. 12). This contrasts
 509 with previous studies that typically calibrate fewer than 12 VIC parameters (e.g., Troy et al., 2008; Isenstein et al., 2015;
 510 Mizukami et al., 2017; Rakovec et al., 2019; Ismail et al., 2020). Options to tackle this more complex calibration problem are
 511 not evaluated here but could include suitable one-step multi-objective optimization algorithms such as PADDs (Asadzadeh et
 512 al. (2014)), or a stepwise multi-objective calibration approach where each set of informative parameters for a specific flux are
 513 adjusted separately (Larabi et al., 2018). Another approach to reduce the complexity of the calibration problem would be
 514 ~~reducing the parameter ranges_ to use a smaller parameter range, which could speed the convergence rate of the search~~
 515 ~~algorithm to the optimal solution. Hence, it would reduce the computation time, but is bearing the risk of optimal values not~~
 516 ~~being included in the too narrow ranges leading to false results~~ However, this would have to be done carefully, possibly
 517 utilizing expert knowledge, in order to ensure the narrower range still contains the optimal solution (Mai, 2023).
 518



519
 520 **Figure 12: Informative parameters (blue) for at least one of simulated streamflow, evapotranspiration, and snow water equivalent.**
 521 **Basin ID description is provided in Table 1.**

522
 523

525 In previous VIC applications, the same parameters are adjusted over large domains to fit the model to streamflow (e.g., Nijssen
526 et al., 2001; Obeidillah et al., 2014; Xue et al., 2015, Mizukami et al., 2017) and against other model output (Isenstein et al.,
527 2015; Ismail et al., 2020) ignoring both the spatial variability of parameter sensitivity and dependence of parameter sensitivity
528 to the hydrological processes. To account for this spatial variability, a multi-site cascading approach (Xue et al., 2015) where
529 calibration parameter selection varies depending on the site can be used. Overall, there remains a need to study how information
530 regarding the spatial variability and process dependence of parameter sensitivity is best integrated into a multi-variable
531 parameter estimation framework.

532 In this study, the low-cost EEE sequential screening method (Cuntz et al., 2105) was used to identify informative parameters.
533 However, this method does not quantitatively rank the importance of these informative parameters. In situations where it is
534 desired to reduce the number of calibration parameters below the counts identified by EEE analyses, a quantitative approach
535 such as variance-based methods (e.g., Sobol', 1990; Saltelli, 2002) or qualitative approach that provides parameter groupings
536 based on their sensitivity could be considered (Sheikholeslami et al., 2019; Mai et al., 2020, 2022). However, future work is
537 required to determine the conditions under which a reduction in the number of calibrated parameters (i.e., by not calibrating
538 some parameters that are informative) could potentially yield better calibration results, particularly in a multi-objective context.

539 **5 Conclusions**

540 Land surface models tend to have large numbers of parameters, many of which cannot be measured directly. Sensitivity
541 analysis is therefore often employed to identify parameters with significant impact on model output variance. Performing
542 sensitivity analysis for large-scale land surface models is, however, computationally demanding. In this study, we consider
543 whether computational cost can be reduced by using watershed classification to transfer information about which parameters
544 sensitively affect streamflow, evapotranspiration and snow water equivalent between basins that have similar climatic and
545 vegetation land cover attributes.

546 The study was performed using a large domain implementation of a hydrologic model as an example. Specifically, we used an
547 updated version of the VIC model (Schnorbus, 2018) that has been coupled to a regional glacier model and implemented across
548 a very large domain in the Pacific Northwest region of North America. A wide range of VIC model parameters was evaluated
549 that include five baseflow parameters, one runoff parameter, nine drainage parameters, four climate parameters, six snow-
550 related parameters, three glacier parameters, and 17 vegetation related parameters. The sensitivity analysis was performed over
551 25 basins spanning a range of hydroclimatic conditions to understand the spatial variability of parameter sensitivities with
552 regard to streamflow, evapotranspiration and snow water equivalent. Parameter sensitivities for each model output were found
553 to vary in a predictable way with basin climate and land cover characteristics.

554 Watershed classification was employed to classify the 25 basins into homogenous groups based on climatic attributes (aridity
555 and snow index) and percentage of glacier area and vegetation land cover. This classification was used to transfer sensitive
556 parameters to each basin based on its group membership. This approach was shown to be able to efficiently identify sensitive
557 parameters with a median *FI* score of 0.87 for streamflow, 0.83 for evapotranspiration and 0.95 for snow water equivalent.
558 These findings suggest that parameter sensitivity can be performed by classifying watersheds into broad groups and then
559 analyzing sensitivity for only a subset of the basins in each group. In our large domain example, we found that it would likely
560 be sufficient to perform sensitivity analysis in 4 % (or fewer) of the basins contained within the domain. This would
561 substantially reduce the cost of the sensitivity analyses that are used to determine the model calibration strategy, or for a given
562 computing budget, would enable the consideration of a broader range of parameters than could be considered if sensitivity
563 analysis were to be performed across the entire domain.

564 The parameter classification based on parameter sensitivities informs which parameters should be adjusted (invariant-
565 informative and variant-informative) depending on the calibration variables that are considered and the local climatic
566 conditions. We found that for a multi-variable calibration approach targeting streamflow, evapotranspiration and snow water
567 equivalent, an average of 77 % of VIC parameters (i.e., 34 of 44 parameters analyzed) were identified as calibration candidates.
568 These parameters include not only those that control runoff and baseflow generation, but also parameters that control snow
569 processes and describe vegetation properties. The findings of this study highlight the need to explore efficient ways to decrease
570 the complexity of multi-process-based calibration of land surface models arising from the increased dimensionality of both the
571 parameter and objective function spaces.

572 Finally, we note that more specific modelling objectives, such as the skillful representation of peaks flows (for flood forecasting
573 purposes), or low flows (for predicting summer drought impacts) could also be considered using the approach that has been
574 proposed. Similarly, the results and methods are applicable to other land surface models.

575 **Code availability**

576 Code of Efficient Elementary Effects (EEE) method is freely available with documentation and examples at
577 <https://doi.org/10.5281/zenodo.3620895>

578 **Author contributions**

579 The study conception was performed by SL, MS and FZ. Sensitivity analysis methodology and code were handled by JM.
580 Formal analysis, investigation and writing original draft were performed by SL. All authors contributed to the writing-review
581 and editing of the manuscript.

582

583 **Competing interests**

584 The authors declare that they have no conflict of interest.

585 **Acknowledgments**

586 Financial support from the Canada First Research Excellence Fund and the Global Water Futures (GWF) program is gratefully
587 acknowledged.

588 **References**

589 Andreadis, K., Storck, P., and Lettenmaier, D. P.: Modeling snow accumulation and ablation processes in forested
590 environments, *Water Resour. Res.*, 45, W05429, doi:10.1029/2008WR007042, 2009.

591 Asadzadeh, M., Tolson, B. A., and Burn, D. H.: A new selection metric for multiobjective hydrologic model calibration, *Water*
592 *Resour. Res.*, 50, 7082–7099, doi:10.1002/2013WR014970, 2014.

593 Bao, Z., Zhang, J., Liu, J., Fu, G., Wang, G., He, R., Yan, X., Jin, J., and Liu, H.: Comparison of regionalization approaches
594 based on regression and similarity for predictions in ungauged catchments under multiple hydro-climatic conditions, *J.*
595 *Hydrol.*, 466–467(1), 37–46, 2012.

596 Baret, F., Weiss, M., Lacaze, R., Camacho, F., Makhmara, H., Pacholczyk, P., and Smets, B.: GEOV1: LAI and FAPAR
597 essential climate variables and FCOVER global time series capitalizing over existing products. Part I: Principles of
598 development and production, *Remote Sens. Environ.*, 137, 299–309, doi:10.1016/j.rse.2012.12.027, 2013.

599 Beck, H. E., Van Dijk, A. I. J. M., De Roo, A., Miralles, D. G., McVicar, T. R., Schellekens, J., and Bruijnzeel, L. A.: Global-
600 scale regionalization of hydrologic model parameters, *Water Resour. Res.*, 52, 3599–3622, doi:10.1002/2015WR018247,
601 2016.

602 Bennett, K. E., Werner, A. T., and Schnorbus, M.: Uncertainties in Hydrologic and Climate Change Impact Analyses in
603 Headwater Basins of British Columbia, *Journal of Climate*, 25, 5711–5730, <https://doi.org/10.1175/JCLI-D-11-00417.1>,
604 2012.

605 Bennett, K. E., Urrego Blanco, J. R., Jonko, A., Bohn, T. J., Atchley, A. L., Urban, N. M., and Middleton, R. S.: Global
606 sensitivity of simulated water balance indicators under future climate change in the Colorado Basin, *Water Resources*
607 *Research*, 54, 132–149. <https://doi.org/10.1002/2017WR020471>, 2018.

608 Blandford, T., Humes, K., Harshburger, B., Moore, B., Walden, V., and Ye H.: Seasonal and synoptic variations in near-
609 surface air temperature lapse rates in a mountainous basin, *J. Appl. Meteorol. Climatol.*, 47(1), 249–261,
610 doi:10.1175/2007JAMC1565.1, 2008.

611 Bohn, T. J., and Vivoni, E. R.: Process-based characterization of evapotranspiration sources over the North American monsoon
612 region, *Water Resources Research*, 52, 358–384. <https://doi.org/10.1002/2015WR017934>, 2016.

613 Boscarello, L., Ravazzani, G., Cislighi, A. and Mancini, M.: Regionalization of Flow-Duration Curves through Catchment
614 Classification with Streamflow Signatures and Physiographic-Climate Indices, *J. Hydrol. Eng.*, 21(3), doi:
615 10.1061/(ASCE)HE .1943-5584.0001307, 2016.

616 Camacho, F., J. Cernicharo, R. Lacaze, F. Baret, and Weiss, M.: GEOV1: LAI, FAPAR essential climate variables and
617 FCOVER global time series capitalizing over existing products. Part 2: Validation and intercomparison with reference
618 products, *Remote Sens. Environ.*, 137, 310–329, doi:10.1016/j.rse.2013.02.030, 2013.

619 Campolongo, F., Cariboni, J., and Saltelli, A.: An effective screening design for sensitivity analysis of large models, *Environ.*
620 *Model. Softw.*, 22, 1509–1518, doi: <https://doi.org/10.1016/j.envsoft.2006.10.004>, 2007.

621 Cherkauer, K. A., Bowling, L. C., and Lettenmaier, D. P.: Variable infiltration capacity cold land process model updates, *Glob.*
622 *Planet. Change*, 38, 151–159, doi: 10.1016/S0921-8181(03)00025- 0, 2003.

623 Choudhury, B. J., and Monteith, J. L.: A four-layer model for the heat budget of homogeneous land surfaces, *Q. J. R. Meteorol.*
624 *Soc.*, 114, 373–398, doi:10.1002/qj.49711448006, 1988.

625 Chicco, D. and Jurman, G.: The advantages of the Matthews correlation coefficient (MCC) over F1 score and accuracy in
626 binary classification evaluation, *BMC Genomics*, 21:6, doi: <https://doi.org/10.1186/s12864-019-6413-7>, 2020.

627 Córdova, M., Célleri, R., Shellito, C.J. et al.: Near-surface air temperature lapse rate over complex terrain in the Southern
628 Ecuadorian Andes: implications for temperature mapping, *Arctic, Antarctic, and Alpine Research*, 48, No.4, pp. 673–684,
629 doi: <http://dx.doi.org/10.1657/AAAR0015-077>, 2016.

630 Compo, G. P., and Coauthors: The Twentieth Century Reanalysis Project, *Q. J. R. Meteorol. Soc.*, 137, 1–28, doi:
631 <https://doi.org/10.1002/qj.776>, 2011.

632 Cuntz, M., et al. Computationally inexpensive identification of noninformative model parameters by sequential screening,
633 *Water Resour. Res.*, 51, 6417–6441, doi: 10.1002/2015WR016907, 2015.

634 Cuntz, M., Mai, J., Samaniego, L., Clark, M., Wulfmeyer, V., Branch, O., Attinger, S., and Thober, S.: The impact of standard
635 and hard-coded parameters on the hydrologic fluxes in the Noah-MP land surface model, *J. Geophys. Res. Atmos.*, 1-25,
636 doi: [http://doi.org/10.1002/\(ISSN\)2169-8996](http://doi.org/10.1002/(ISSN)2169-8996), 2016.

637 Danielson, J. J., and Gesch, D. B.: Global Multi-resolution Terrain Elevation Data 2010 (GMTED2010), U.S. Geological
638 Survey, Reston, Virginia, <http://pubs.usgs.gov/of/2011/1073/pdf/of2011-1073.pdf> (Accessed November 2, 2015), 2011.

639 Demaria, E. M., Nijssen, B., and Wagener, T.: Monte Carlo sensitivity analysis of land surface parameters using the Variable
640 Infiltration Capacity model, *J. Geophys. Res.*, 112, D11113, doi:10.1029/2006JD007534, 2007.

641 Demirel, M. C., Mai, J., Mendiguren, G., Koch, J., Samaniego, L., and Stisen, S.: Combining satellite data and appropriate
642 objective functions for improved spatial pattern performance of a distributed hydrologic model, *Hydrology and Earth*
643 *System Sciences*, 22(2), 1299–1315, doi: <http://doi.org/10.5194/hess-22-1299-2018>, 2018.

644 Devak, M. and Dhanya, C.T.: Sensitivity analysis of hydrological models: review and way forward, *Journal of Water and*
645 *Climate Change*, doi: 10.2166/wcc.2017.149, 2017.

646 Dickinson, R. E.: Land surface processes and climate - surface albedos and energy balance, *Theory of Climate*, B. Saltzman,
647 Ed., Vol. 25 of *Advances in Geophysics*, Academic Press, Inc., New York, NY, 305–353, 1983.

648 Ducoudré, N. I., Laval, K., and Perrier A.: SECHIBA, a New Set of Parameterizations of the Hydrologic Exchanges at the
649 Land-Atmosphere Interface within the LMD Atmospheric General Circulation Model, *J. Clim.*, 6, 248–273,
650 doi:10.1175/1520-0442(1993)0062.0.CO2, 1993.

651 Euser, T., Winsemius, H.C., Hrachowitz, M., Fencia, F., Uhlenbrook, S. and Savenije, H.H.G.: A framework to assess the
652 realism of model structures using hydrological signatures, *Hydrol. Earth Syst. Sci.*, 17, 1893-1912, 2013.

653 Fitzpatrick, N., Radić, V., and Menounos, B.: A multi-season investigation of glacier surface roughness lengths through in situ
654 and remote observation. *The Cryosphere*, 13, 1051–1071, doi: <https://doi.org/10.5194/tc-13-1051-2019>, 2019.

655 Francini, M., and Pacciani, M.: Comparative-analysis of several conceptual rainfall runoff models, *Journal of Hydrology*,
656 122(1-4), 161-219, 1991.

657 Gao, H. et al.: Water Budget Record from Variable Infiltration Capacity (VIC) Model, In *Algorithm Theoretical Basis*
658 *Document for Terrestrial Water Cycle Data Records* (unpublished), 2009.

659 Garambois, P. A., Roux, H., Larnier, K., Labat, D., and Dartus, D.: Parameter regionalization for a process-oriented distributed
660 model dedicated to flash floods, *J. Hydrol.*, 525, 383–399, doi: 10.1016/j.jhydrol.2015.03.052, 2015.

661 Grenfell, T. C.: Albedo, *Encyclopedia of Snow, Ice and Glaciers*, V.P. Singh, P. Singh, and U.K. Haritashya, Eds., Springer
662 Netherlands, 23–35, 2011.

663 Göhler, M., Mai, J., and Cuntz, M.: Use of eigen decomposition in a parameter sensitivity analysis of the Community Land
664 Model, *Journal of Geophysical Research: Biogeosciences*, 118(2), 904–921, doi: <http://doi.org/10.1002/jgrg.20072>, 2013.

665 Gou, J., Miao, C., Duan, Q., Tang, Q., Di, Z., Liao, W., et al.: Sensitivity analysis-based automatic parameter calibration of
666 the VIC model for streamflow simulations over China, *Water Resources Research*, 56, e2019WR025968, doi:
667 <https://doi.org/10.1029/2019WR025968>, 2020.

668 Hamlet AF, and Lettenmaier. DP.: Effects of climate change on hydrology and water resources in the Columbia River Basin,
669 *Journal of the American Water Resources Association*, 35,6, 1999.

670 He, Y., Bardossy, A. and Zehe, E.: A review of regionalisation for continuous streamflow simulation, *Hydrol. Earth Syst. Sci.*,
671 15, 3539–3553, doi: 10.5194/hess-15-3539-2011, 2011.

672 He, R., and Pang B.: Sensitivity and uncertainty analysis of the Variable infiltration Capacity model in the upstream of Heihe
673 River basin, *Proc. Int. Assoc. Hydrol. Sci.*, 8 (4), 312–316, doi: <https://doi.org/10.2166/wcc.2017.149>, 2014.

674 He, Z.H., Tian, F.Q., Gupta, H., Hu, H.C., Hu, H.P.: Diagnostic calibration of a hydrological model in a mountain area by
675 hydrograph partitioning, *Hydrol Earth Syst. Sci.*, 19, 1807–1826, 2015.

676 Herman, J.D., Kollat, J.B., Reed, P.M. and Wagener, T.: Technical Note: Method of Morris effectively reduces the
677 computational demands of global sensitivity analysis for distributed watershed models, *Hydrol. Earth Syst. Sci.*, 17, 2893–
678 2903, doi: 10.5194/hess-17-2893-2013, 2013.

679 Hou, Z., Huang, M., Leung, L. R., Lin, G., and Ricciuto, D. M.: Sensitivity of surface flux simulations to hydrologic parameters
680 based on an uncertainty quantification framework applied to the Community Land Model, *J. Geophys. Res.*, 117, D15108,
681 doi: 10.1029/2012JD017521, 2012.

682 Houle, E.S. Livneh, B. and Kasprzyk, J.R.: Exploring snow model parameter sensitivity using Sobol' variance decomposition,
683 *Environmental Modelling & Software*, 89, 144-158, 2017.

684 Hornberger, G., and Spear, R.: An approach to the preliminary analysis of environmental systems, *J. Environ. Manage.*, 12,
685 7– 18, 1981.

686 Isenstein, E.M., Wi, S. Yang, Y.C. and Brown, C.: Calibration of a Distributed Hydrologic Model Using Streamflow and
687 Remote Sensing Snow Data, *World Environmental and Water Resources Congress 2015*, 2015.

688 Islam, SU, Déry, S and Werner, A.T.: Future Climate change Impacts on Snow and Water Resources of the Fraser River Basin,
689 British Columbia, *Journal of Hydrometeorology*, doi: 10.1175/JHM-D-16-0012.1, 2017.

690 Ismail, M.F., Naz, B.S., Wortmann, M. et al.: Comparison of two model calibration approaches and their influence on future
691 projections under climate change in the Upper Indus Basin, *Climatic Change*, 163, 1227–1246, doi:
692 <https://doi.org/10.1007/s10584-020-02902-3>, 2020.

693 Jackson, R. B., J. Canadell, J. R. Ehleringer, H. A. Mooney, O. E. Sala, and Schulze, E. D. : A global analysis of root
694 distributions for terrestrial biomes, *Oecologia*, 108, 389–411, doi:10.1007/BF00333714, 1996.

695 Jafarzadegan, K. Merwade, V. and Moradkhani, H.: Combining clustering and classification for the regionalization of
696 environmental model parameters: Application to floodplain mapping in data-scarce regions, *Environmental Modelling and
697 Software*, 125, doi: <https://doi.org/10.1016/j.envsoft.2019.104613>, 2020.

698 Jiskoot, H. and Mueller, M.S.: Glacier fragmentation effects on surface energy balance and runoff: field measurements and
699 distributed modelling, *Hydrol. Process.*, 26, 1861–1875, 2012.

700 Jost, F., Moore, RD, Menounos, B and Wheate, R.: Quantifying the contribution of glacier runoff to streamflow in the upper
701 Columbia River Basin, Canada, *Hydrol. Earth Syst. Sci.*, 16, 849–860, 2012.

702 Kanishka, G. and Eldho, T.I.: Streamflow estimation in ungauged basins using watershed classification and regionalization
703 techniques, *J. Earth Syst. Sci.*, 129,186, doi: <https://doi.org/10.1007/s12040-020-01451-8>, 2020.

704 Kienzle, S. W.: A new temperature based method to separate rain and snow, *Hydrol. Process.*, 22, 5067–5085, doi:
705 <https://doi.org/10.1002/hyp.7131>, 2008.

706 Kuhn, M., 2003. Redistribution of snow and glacier mass balance from a hydrometeorological model, *Journal of Hydrology*,
707 282, 95–103, doi: [https://doi.org/10.1016/S0022-1694\(03\)00256-7](https://doi.org/10.1016/S0022-1694(03)00256-7).

708 Lafleur, P.: Leaf conductance of four species growing in a subarctic marsh, *Can. J. Bot.*, 66, 1367– 1375, doi: 10.1139/b88-
709 192, 1988.

710 Larabi, S., St-Hilaire, A., Chebana, F. and Latraverse, M.: Multi-Criteria Process-Based Calibration Using Functional Data
711 Analysis to Improve Hydrological Model Realism, *Water Resour Manage.*, 32, 195–211, doi: 10.1007/s11269-017-1803-6,
712 2018.

713 Levia, D.F., Nanko, K., Amasaki, H. et al.: Throughfall partitioning by trees, *Hydrol. Process.*, 33, 1698-1708, 2019.

714 Liang, X., Lettenmaier, D. P., Wood, E. F., and Burges S. J.: A simple hydrologically based model of land-surface water and
715 energy fluxes for general-circulation models, *J. Geophys. Res. Atmospheres*, 99, 14415–14428, doi: 10.1029/94JD00483,
716 1994.

717 Lilhare, R. Pokorný, S. Déry, S.J., Stadynek, T.A. and Koenig, K. A.: Sensitivity analysis and uncertainty assessment in water
718 budgets simulated by the variable infiltration capacity model for Canadian subarctic watersheds, *Hydrological Processes*,
719 34, 2057–2075, doi: 10.1002/hyp.13711, 2020.

720 Liang, X., Wood, E. F., and Lettenmaier D. P.: Surface soil moisture parameterization of the VIC-2L model: Evaluation and
721 modification, *Glob. Planet. Change*, 13, 195–206, doi: 10.1016/0921- 8181(95)00046-1, 1996.

722 Lohmann, D., Raschke, E., Nijssen, B. and Lettenmaier, D.P.: Regional scale hydrology: II. Application of the VIC-2L model
723 to the Weser River, Germany, *Hydrological Sciences Journal*, 43:1, 143-158, doi: 10.1080/02626669809492108, 1998.

724 Mai, J. (2023). Ten strategies towards successful calibration of environmental models. *Journal of Hydrology*, 620(A),
725 129414. <http://doi.org/https://doi.org/10.1016/j.jhydrol.2023.129414>
726

727 Mai, J. and Cuntz M.: Computationally inexpensive identification of noninformative model parameters by sequential
728 screening: Efficient Elementary Effects (EEE) (v1.0), Zenodo <https://doi.org/10.5281/zenodo.3620895>., 2020.

729 Mai, J., Craig, J. R., and Tolson, B. A.: Simultaneously determining global sensitivities of model parameters and model
730 structure, *Hydrology and Earth System Sciences*, 24(12), 5835–5858, doi: <http://doi.org/10.5194/hess-24-5835-2020>,
731 2020.

732 Mai, J., Arsenault, R., Tolson, B. A., Latraverse, M., and Demeester, K.: Application of parameter screening to derive optimal
733 initial state adjustments for streamflow forecasting, *Water Resources Research*, 56(9), e2020WR027960, 2020.

734 Mai, J., Craig, J. R., Tolson, B. A., and Arsenault, R.: The sensitivity of simulated streamflow to individual hydrologic
735 processes across North America, *Nature Communications*, 13(1), 455, doi: <http://doi.org/10.1038/s41467-022-28010-7>,
736 2022.

737 Marshall, S.J., White, E.C., Demuthm M.D et al.: Glacier Water Resources on the Eastern Slopes of the Canadian Rocky
738 Mountains, *Canadian Water Resources Journal*, 36:2, 109-134, doi: 10.4296/cwrj3602823, 2011.

739 Matheussenm, B., Kirschsbaum, R.L., Goodman, I.A., O'Donnell, G.M., and Lettenmaier, D.P.: Effects of land cover change
740 on streamflow in the interior Columbia River Basin (USA and Canada), *Hydrol. Process*, 14, 867-885, 2000.

741 Melsen, L., Teuling, A., Torfs, P. Zappa, M. et al.: Representation of spatial and temporal variability in large-domain
742 hydrological models: case study for a mesoscale pre-Alpine basin, *Hydrol. Earth Syst. Sci.*, 20, 2207–2226, doi:
743 10.5194/hess-20-2207-2016, 2016.

744 Mendoza, P. A., Clark, M. P., Barlage, M., Rajagopalan, B., Samaniego, L., Abramowitz, G., and Gupta, H.: Are we
745 unnecessarily constraining the agility of complex process-based models?, *Water Resour. Res.*, 51 (1), 716– 728, doi:
746 <http://doi.org/10.1002/2014WR015820>, 2015.

747 Morris, M.D.: Factorial sampling plans for preliminary computational experiments, *Technometrics*, 33 (2), 161e174, doi:
748 <http://dx.doi.org/10.2307/1269043>, 1991.

749 Minder, J. R., Mote, P. W., and Lundquist, J. D.: Surface temperature lapse rates over complex terrain: Lessons from the
750 Cascade Mountains, *J. Geophys. Res.*, 115, D14122, doi: 10.1029/2009JD013493, 2010.

751 Mizukami, N., Clark, M.P., Newman, A.J. Wood, A.W, Gutmann, E.D, Nijssen, B., Rakovec, O. and Samaniego, L.: Towards
752 seamless large-domain parameter estimation for hydrologic models, *Water Resour. Res.* 53, 8020-8040, doi:
753 10.1002/2017WR020401, 2017.

754 Munro, D. S.: Stomatal conductances and surface conductance modelling in a mixed wetland forest, *Agric. For. Meteorol.*, 48,
755 235–249, doi: 10.1016/0168-1923(89)90071-3, 1989.

756 Nasanova, O.N., Gusev, M.Y. and Kovalev, Y.: Investigating the Ability of a Land Surface Model to Simulate Streamflow
757 with the Accuracy of Hydrological Models: A Case Study Using MOPEX Materials, *Journal of Hydrometeorology*, 10,
758 1128-1150, doi: 10.1175/2009JHM1083.1, 2009.

759 Nijssen, B., O'Donnell, G.M., Lettenmaier, D.P., Lohmann, D., Wood, E.F.: Predicting the discharge of global rivers, *J. Clim.*
760 14 (15), 3307e3323, 2001.

761 Oudin, L., Andréassian, V., Perrin, C., Michel, C. and Le Moine, N.: Spatial proximity, physical similarity, regression and
762 unged catchments: A comparison of regionalization approaches based on 913 French catchments, *Water Resources*
763 *Research*, 44, W03413, doi: 10.1029/2007WR006240, 2008.

764 Oubeidillah, A.A., Kao, S.C., Ashfaq, M., Naz, B.S. and Tootle, G.: A large-scale, high-resolution hydrological model
765 parameter data set for climate change impact assessment for the conterminous US, *Hydrol. Earth Syst. Sci.*, 18, 67–84, doi:
766 10.5194/hess-18-67-2014, 2014.

767 Payne, J.T., Wood A.W., Hamlet, A.F., Palmer, R.N., and Lettenmaier, D.P.: Mitigating the effects of climate change on the
768 water resources of the Columbia River basin, *Climatic Change*, 62: 233–256, 2004.

769 Pelletier, J.D., Broxton, P.D., Hazenberg, P., Zeng, X., Troch, P.A., Niu, G., Williams, Z.C., Brunke, M.A., and Gochis, D.:
770 Global 1-km Gridded Thickness of Soil, Regolith, and Sedimentary Deposit Layers. ORNL DAAC, Oak Ridge, Tennessee,
771 USA, doi: <https://doi.org/10.3334/ORNLDAAC/1304>, 2016.

772 Pelto, B.M., Maussion, F., Menounos, B., Radić, V., and Zeuner, M.: Bias corrected estimates of glacier thickness in the
773 Columbia River Basin, Canada, *Journal of Glaciology*, 66(260), 1051–1063, doi: <https://doi.org/10.1017/jog.2020.75>,
774 2020.

775 Pianosi, F., Beven, K., Freer, J., Hall, J.W., Rougier, J., Stephenson, D.B., and Wagener, T.: Sensitivity analysis of
776 environmental models: A systematic review with practical workflow, *Environmental Modelling & Software*, 79, 214-232,
777 2016.

778 Razavi, T. and Coulibaly, P.: Streamflow Prediction in Ungauged Basins: Review of Regionalization Methods, *J. Hydrol.*
779 *Eng.*, 18, 8, 958-975, doi: 10.1061/(ASCE) HE.1943-5584.0000690, 2013.

780 Rakovec, O., Kumar, R., Attinger, S. and Samaniego, L.: Improving the realism of hydrologic model functioning through
781 multivariate parameter estimation, *Water Resour Res*, 52, 7779–7792, doi: <https://doi.org/10.1002/2016WR019430>, 2016.

782 Rakovec, O., Mizukami, N., Kumar, R., Newman, A., Thober, S., Wood, A. W., et al.: Diagnostic evaluation of large-domain
783 hydrologic models calibrated across the contiguous United States, *Journal of Geophysical Research: Atmospheres*, 124,
784 13,991–14,007, doi: <https://doi.org/10.1029/2019JD030767>, 2019.

785 Rosero, E., Yang, Z.L., Wagener, T., Gulden, L. E., Yatheendradas, S., and Niu, G.Y.: Quantifying parameter sensitivity,
786 interaction, and transferability in hydrologically enhanced versions of the Noah land surface model over transition zones
787 during the warm season, *J. Geophys. Res.*, 115, D03106, doi:10.1029/2009JD012035, 2010.

788 Roux, M.: A Comparative Study of Divisive and Agglomerative Hierarchical Clustering Algorithms, *Journal of Classification*,
789 35, 345-366, doi: 10.1007/s00357-018-9259-9, 2018.

790 Samaniego, L., Kumar, R., and Attinger, S.: Multiscale parameter regionalization of a grid-based hydrologic model at the
791 mesoscale, *Water Resour. Res.*, 46, W05523, doi:10.1029/2008WR007327, 2010.

792 Samuel, J., Coulibaly, P., and Metcalfe, R.: Estimation of continuous streamflow in Ontario ungauged basins: Comparison of
793 regionalization methods, *J. Hydrol. Eng.*, 16(5), 447–459, 2011.

794 Saltelli, A.: Making best use of model valuations to compute sensitivity indices, *Comput. Phys. Commun.*, 145 (2), 280e297,
795 doi: [http://dx.doi.org/10.1016/S0010-4655\(02\)00280-1](http://dx.doi.org/10.1016/S0010-4655(02)00280-1), 2002.

796 Saltelli, A., Ratto, M., Andres, T., Campolongo, F., Cariboni, J., Catelli, D., Saisana, M., Tarantola, S.: *Global Sensitivity*
797 *Analysis, The Primer* Wiley, 2008.

798 Sarrazin, F. Pianosi, F. and Wagener, T.: Global Sensitivity Analysis of environmental models: Convergence and validation,
799 *Environmental Modelling & Software*, 79, 135-152, 2016.

800 Sawicz, K., Wagener, T., Sivapalan, M., Troch, P.A. and Carrillo, G.: Catchment classification: empirical analysis of
801 hydrologic similarity based on catchment function in the eastern USA, *Hydrol. Earth Syst. Sci. Discuss.*, 8, 4495–4534,
802 doi: 10.5194/hessd-8-4495-2011, 2011.

803 Schnorbus, M. A.: VIC-Glacier (VIC-GL): Description of VIC Model Changes and Upgrades, VIC Generation 2 Deployment
804 Report, Volume 1, Pacific Climate Impacts Consortium, University of Victoria, Victoria, BC, 40 pp, 2018.

805 Shafii, M. and Tolson, B. A.: Optimizing hydrological consistency by incorporating hydrological signatures into model
806 calibration objectives, *Water Resour. Res.*, doi: 10.1002/2014WR016520, 2015.

807 Shafii, M., Basu, N., Craig, J.R., Schiff, S.L., and Van Cappellen, P.: A diagnostic approach to constraining flow partitioning
808 in hydrologic models using a multiobjective optimization framework, *Water Resour Res.*, doi:
809 <https://doi.org/10.1002/2016WR019736>, 2017.

810 Schenk, H. J., and Jackson, R. B.: The global biogeography of roots, *Ecol. Monogr.*, 72, 311–328, doi: 10.1890/0012-
811 9615(2002)072[0311:TGBOR]2.0.CO2, 2002.

812 Schnorbus, M. A., Bennett, K.E., Werner, A.T., and Berland, A.J.: Hydrologic Impacts of Climate Change in the Peace,
813 Campbell and Columbia Watersheds, British Columbia, Canada, Pacific Climate Impacts Consortium, University of
814 Victoria: Victoria, BC, 2011.

815 Schnorbus, M. A., Werner, A., and Bennett, K.: Impacts of climate change in three hydrologic regimes in British Columbia,
816 Canada, *Hydrol. Process.*, 28, 1170–1189, doi: <https://doi.org/10.1002/hyp.9661>, 2014.

817 Sellers, P. J.: Canopy reflectance, photosynthesis and transpiration, *Int. J. Remote Sens.*, 6, 1335– 1372, doi:
818 10.1080/01431168508948283, 1985.

819 Sepúlveda, U.M., Mendoza, P.A., Mizukami, N. and Newman, A.J.: Revisiting parameter sensitivities in the Variable
820 Infiltration Capacity model, *Hydrology and Earth System Sciences Discussions*, doi: [https://doi.org/10.5194/hess-2021-](https://doi.org/10.5194/hess-2021-550)
821 550, 2021.

822 Sheikholeslami, R., Razavi, S., Gupta, H.V., Becker, W. and Haghnegahdar, A.: Global sensitivity analysis for high-
823 dimensional problems: How to objectively group factors and measure robustness and convergence while reducing
824 computational cost, *Environmental Modelling & Software* 111, 282-299, 2019.

825 Shrestha, R.R., Schnorbus, M. A., Werner, A.T. and Berland, A.J.: Modelling spatial and temporal variability of hydrologic
826 impacts of climate change in the Fraser River basin, British Columbia, Canada, *Hydrol. Process.*, 26, 1840–1860, 2012.

827 Shrestha, R. R., Cannon, A. J., Schnorbus, M. A., and Zwiers, F. W.: Projecting future nonstationary extreme streamflow for
828 the Fraser River, Canada, *Climatic Change*, 145, 289–303, doi: <https://doi.org/10.1007/s10584-017-2098-6>, 2017.

829 Shrestha, R. R., Cannon, A. J., Schnorbus, M. A., and Alford, H.: Climatic Controls on Future Hydrologic Changes in a
830 Subarctic River Basin in Canada, *J. Hydrometeor.*, 20, 1757–1778, doi: <https://doi.org/10.1175/JHM-D-18-0262.1>, 2019.

831 Schulze, E.-D., Kelliher, F. M., Korner, C., Lloyd, J., and Leuning, R.: Relationships among maximum stomatal conductance,
832 ecosystem surface conductance, carbon assimilation rate, and plant nitrogen nutrition: A global ecology scaling exercise,
833 *Annu. Rev. Ecol. Syst.*, 25, 629–660, 1994.

834 Shin, M-J, Guillaume, J.H.A., Croke, B.F.W., and Jakeman, A. J.: Addressing ten questions about conceptual rainfall–runoff
835 models with global sensitivity analyses in *R. Journal of Hydrology* 503,135–152, 2013.

836 Simard, M., Pinto, N., Fisher, J. B., and Baccini, A.: Mapping forest canopy height globally with spaceborne lidar, *J. Geophys.*
837 *Res. Biogeosciences*, 116, G04021, doi: 10.1029/2011JG001708, 2011.

838 Sobol', I.M.: Sensitivity estimates for nonlinear mathematical models, *Matematicheskoe Modelirovanie* 2, 112-118 (in
839 Russian), translated in English (1993), In: *Mathematical Modelling and Computational Experiments*, 1(4), pp. 407-414,
840 1990.

841 Toney, C., and Reeves, M. C.: Equations to convert compacted crown ratio to uncompact crown ratio for trees in the Interior
842 West, *Western Journal of Applied Forestry*, 24(2), 76–82, 2009.

843 Troy, T.J., Wood, E.F. and Sheffield J.: An efficient calibration method for continental-scale land surface modelling, *Water*
844 *Resour. Res.* 44, W09411, doi: 10.1029/2007WR006513, 2008.

845 Van Griensven, A., Meixner, T., Grunwald, S., Bishop, T., Diluzio, M., and Srinivasan, R.: A global sensitivity analysis tool
846 for the parameters of multi-variable catchment models, *Journal of Hydrology*, 324(1), 10–23, 2006.

847 Vihma, T.: Atmosphere-Snow/Ice Interactions. *Encyclopedia of Snow, Ice and Glaciers*, V.P. Singh, P. Singh, and U.K.
848 Haritashya, Eds., Springer Netherlands, 66–75, 2011.

849 Waheed, S.Q., Grigg, N.S., Ramirez, J.A.: Variable Infiltration-Capacity Model Sensitivity, Parameter Uncertainty, and Data
850 Augmentation for the Diyala River Basin in Iraq, *J. Hydrol. Eng.*, 25(9), doi: 10.1061/(ASCE)HE.1943-5584.0001975,
851 2020.

852 Wang, T.L., Hamann, A., Spittlehouse, D.L., Murdock, T.Q.: ClimateWNA--High-Resolution Spatial Climate Data for
853 Western North America, *Journal of Applied Meteorology and Climatology*, 51 (1), 16–29, doi: 10.1175/JAMC-D-11-
854 043.1, 2012

855 Wallner, M., Haberlandt, U., and Dietrich, J.: A one-step similarity approach for the regionalization of hydrological model
856 parameters based on self-organizing maps, *J. Hydrol.*, 494, 59–71, doi: 10.1016/j.jhydrol.2013.04.022, 2013.

857 Wenger, S. J., Luce, C. H., Hamlet, A. F., Isaak, D. J., and Neville, H. M.: Macroscale hydrologic modeling of ecologically
858 relevant flow metrics, *Water Resour. Res.*, 46, W09513, doi: 10.1029/2009WR008839, 2010.

859 Werner, A. T., Schnorbus, M. A., Shrestha, R. R., Cannon, A. J., Zwiers, F. W., Dayon, G. and Anslow, F.: A long-term,
860 temporally consistent, gridded daily meteorological dataset for northwestern North America, *Sci. Data*, 6, 180299, 2019.

861 Woods, R.A.: Analytical model of seasonal climate impacts on snow hydrology: Continuous snowpacks, *Advances in Water*
862 *Resources*, 32, 1465-1481, doi: 10.1016/j.advwatres.2009.06.011, 2011.

863 Xie Z. and Yuan, F.: A parameter estimation scheme of the land surface model VIC using the MOPEX databases, *Large*
864 *Sample Basin Experiments for Hydrological Model Parameterization: Results of the Model Parameter Experiment–*
865 *MOPEX. IAHS Publ. 307*, 2006.

866 Xue, X., Zhang, K., Hong, Y. et al.: New Multisite Cascading Calibration Approach for Hydrological Models: Case Study in
867 the Red River Basin Using the VIC Model, *J. Hydrol. Eng.*, 2016, 21(2): doi: 10.1061/(ASCE)HE.1943-5584.0001282.,
868 2015.

869 Yadav, M., Wagener, T., Gupta, H.: Regionalization of constraints on expected watershed response behavior for improved
870 predictions in ungauged basins. *Advances in Water Resources*, 30, 1756–1774, 2007.

871 Yanto, Livneh, B. Rajagopalan, B. and Kasprzyk, J.: Hydrological model application under data scarcity for multiple
872 watersheds, Java Island, Indonesia, *Journal of Hydrology: Regional Studies*, 9, 127–139, doi:
873 <https://doi.org/10.1016/j.ejrh.2016.09.007>, 2017.

874 Yilmaz, K. K., Gupta, H. V. and Wagener, T.: A process-based diagnostic approach to model evaluation: Application to the
875 NWS distributed hydrologic model, *Water Resour. Res.*, W09417, doi: 10.1029/2007WR006716, 2008.

876 Young, P.C., Spear, R.C., Hornberger, G.M.: Modelling badly defined systems: some further thoughts. In: *Proceedings*
877 *SIMSIG Conference, Canberra*, pp. 24-32, 1978.

878